Marine Geology 303–306 (2012) 137–153

Contents lists available at SciVerse ScienceDirect

Marine Geology

journal homepage: www.elsevier.com/locate/margeo

External controls on turbidite sedimentation on the glacially-influenced Armorican margin (Bay of Biscay, western European margin)

Samuel Toucanne [a,*], Sebastien Zaragosi [b], Jean-François Bourillet [a], Bernard Dennielou [a], Stephan J. Jorry [a], Gwenael Jouet [a], Michel Cremer [b]

[a] IFREMER, Laboratoire Environnements Sédimentaires, BP70, 29280 Plouzané, France
[b] Université Bordeaux I, UMR 5805, Avenue des Facultés, F-33405 Talence, France

ARTICLE INFO

Article history:
Received 29 July 2011
Received in revised form 20 February 2012
Accepted 21 February 2012
Available online 3 March 2012

Communicated by D.J.W. Piper

Keywords:
Armorican margin
Bay of Biscay
turbidite systems
turbidity currents
levee growth
external forcing
deglaciation
source-to-sink

ABSTRACT

Sequence stratigraphic models predict increased sediment delivery to deep-water areas during sea-level lowstand. The Armorican margin (Bay of Biscay, western European margin) is an interesting area to test this hypothesis because the margin has a wide continental shelf, still partly flooded during sea-level lowstand, and the Armorican turbidite system has experienced fluctuating sediment fluxes since the last glacial period. The stratigraphic response of the Armorican turbidite system to sea-level oscillations and climate changes was assessed for the last 35,000 years through the study of the Guilcher, Crozon and Audierne levees. Millennial-timescale resolution chronostratigraphy allowed us to reconstruct the sediment accumulation and turbidite frequency, thickness and grain-size over this period of time.

We found that the Armorican turbidite system was sediment-starved during highstand conditions (ca. 8–0 ka) and that glacial conditions favoured sediment delivery to the deep Bay of Biscay. However, contrary to what would be expected from sequence stratigraphic models, the turbidite flux did not reach a maximum during the LGM lowstand (ca. 26–20 ka) but at the onset of Termination I (between ca. 20 and 17 ka). This makes the Armorican turbidite system a transgression-dominated one. This sediment pulse can be interpreted as a huge increase in the meltwater discharge of the Fleuve Manche palaeoriver in response to the decay of the British and Fennoscandian ice-sheets. At that time, despite the rising sea-level, a large deltaic system had to have developed on the outer shelf, leading to the delivery of the Fleuve Manche sediment load into the canyon heads. On the other hand, our dataset suggest that the delivery of sediment into canyons was mainly forced by the winnowing and reworking of the sediment stored on the wide, drowned shelf during the last glacial period (between ca. 35 and 20 ka, and between 17 and 8 ka). These findings illustrate the competing influences of accommodation and sediment supply on the Armorican margin over the last 35,000 years, with a shelf acting as a buffer for the sediment supply signal for most of the period, except during the last deglaciation. At that time, the western European sediment-routing system was *reactive*, the climatic signal rapidly propagated from the southern limb of the European ice-sheet to the Armorican turbidite system. Finally, our study demonstrates that precise reconstruction of turbidite flux in deep-water areas, added to knowledge about the morphology of the margin and the palaeoenvironmental changes (fluvial system, shoreline position, etc.), are crucial for determining the response of turbidite systems to external forcing.

1. Introduction

Deep-sea turbidite systems are common sedimentary features in ocean basins, and represent a final sink for sediment flux across continental margins. Their high diversity in morphology, internal structure and composition results from the complex interaction between internal (i.e. autogenic) and external forcings (i.e. allogenic) (Normark et al., 1993; Reading and Richards, 1994). Their development is externally forced by river runoff and sea-level fluctuations. Such depositional systems could, therefore, record long- and short-term climatic oscillations and associated palaeoenvironmental changes (Bouma, 2001), especially if the terrestrial and deep depositional environments respond simultaneously to climate-driven disturbances (*reactive* sediment routing system sensu Allen, 2008).

Recent simulations and experiment-based studies have strongly questioned this hypothesis (Jerolmack and Paola, 2010; Armitage et al., 2011a,b). Firstly, these studies show that terrestrial segments of sediment routing systems (i.e. river, floodplain and river mouth) likely obliterate the expression of high-frequency palaeoenvironmental changes (Jerolmack and Paola, 2010; Armitage et al., 2011b). Secondly, simulations suggest that the development of sediment cycles on continental margins is largely driven by sea-level changes,

* Corresponding author. Tel.: +33 298 22 4249; fax: +33 298 22 4570.
E-mail address: stoucann@ifremer.fr (S. Toucanne).

0025-3227/$ – see front matter © 2012 Elsevier B.V. All rights reserved.
doi:10.1016/j.margeo.2012.02.008

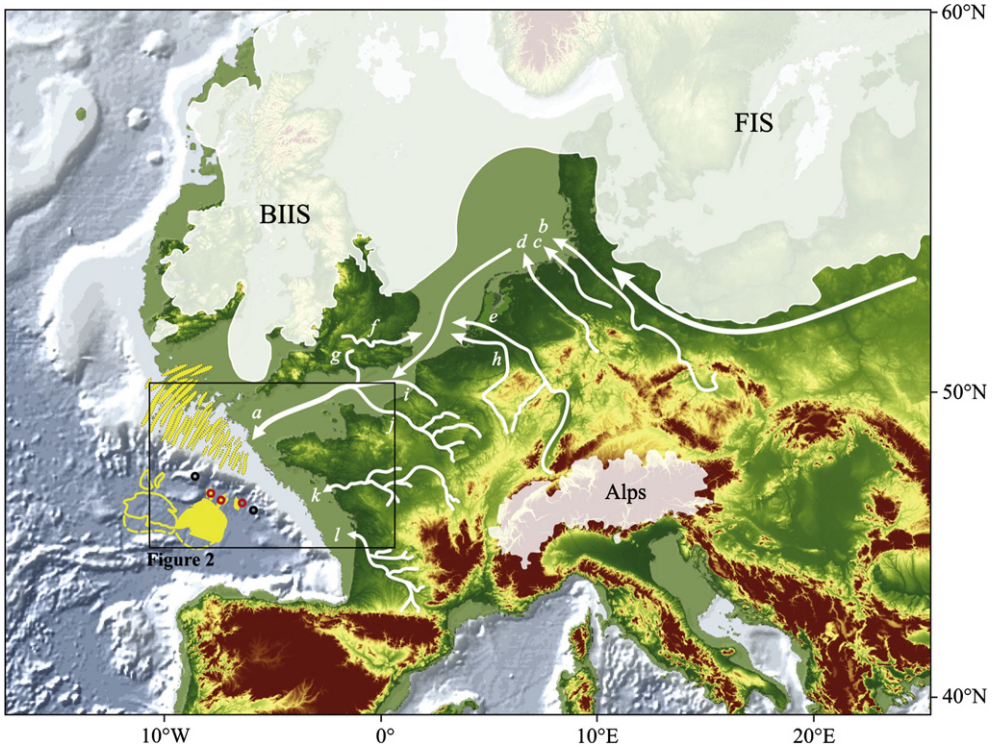

Fig. 1. The Armorican turbidite system (filled yellow area — Bay of Biscay), and the regional palaeogeographical context during the Last Glacial Maximum (LGM, ca. 30–20 ka in Europe) showing the extent of the British Irish Ice Sheet (BIIS), Fennoscandian Ice Sheet (FIS) and the Alps glaciers (white shaded areas) (Ehlers et al., 2011). The thick white arrow parallel to the southernmost part of the FIS depicts the meltwater flow within the Vilnius–Warsaw–Berlin ice-marginal valley. The thin white arrows and the associated lowercase letters indicate the main European rivers: *a*: Fleuve Manche, *b*: Elbe, *c*: Weser, *d*: Ems, *e*: Rhine, *f*: Thames, *g*: Solent, *h*: Meuse, *i*: Somme, *j*: Seine, *k*: Loire, *l*: Gironde. Black and red circles indicate the locations of the cores retrieved in hemipelagic (MD95-2002 and MD03-2696) and turbiditic (MD03-2690, MD03-2688 and MD03-2695) depositional environments (see Fig. 2 for details). The open yellow areas in the deep-sea depict the position of the Celtic Fan (Zaragosi et al., 2000). The distal boundaries of the Celtic and Armorican depositional systems are unknown (Bourillet et al., 2006). The filled yellow areas on the continental shelf indicate the location of the Celtic sand banks (Reynaud et al., 2003).

with the terrestrial sediment supply only playing a minor role (Armitage et al., 2011a). In addition, the lag time between climate-driven onshore changes and offshore deposition might reach millions of years in extensive land-to-deep-sea sediment routing systems (Métivier and Gaudemer, 1999; Castelltort and Van Den Driessche, 2003). However, some recent studies focusing on deep depositional systems and using a high-resolution chronostratigraphic framework, have demonstrated rapid climatic signal propagation from source to sink. For instance, Covault et al. (2010) recently demonstrated that Holocene fluctuations in the precipitation over southern California drove the deep-sea turbidite deposition in the Newport deep-sea depositional system. Jorry et al. (2011) have also shown that glacial oscillations in the southern French Alps at the end of the last glacial period controlled turbidite sedimentation in the Var deep-sea fan. Over a longer time-scale, Nakajima and Itaki (2007) found that changes in turbidite activity in the central Japan Sea are consistent with the terrestrial climatic variability over the last 70 ka. As pointed out by these authors, these are all *reactive* systems because the Newport, Var and Toyama depositional systems are permanently connected to their feeding rivers due to the absence of a well-developed shelf. Sequence stratigraphic models predict that broad continental shelves act as a buffer between the continent and submarine canyon systems during highstand conditions, especially when canyon heads are detached from terrestrial sources. As a result, turbidite sedimentation strengthened during sea-level fall and reached a maximum during sea-level lowstand (Posamentier and Vail, 1988). Recently, Covault and Graham (2010) revised this concept by showing that the majority of continental-margin deep-sea deposition also occurred during periods of marine transgression, especially off decaying ice-sheets (Kolla and Perlmutter, 1993; Skene and Piper, 2003). For instance, the sediment flux in the Mississippi Fan recorded the growth and then decay of the Laurentide ice-sheet, the climatic signal propagating to the slope and the deep Gulf of Mexico during lowstand and rising sea level through cross-shelf valleys and the shelf margin delta (Suter and Berryhill, 1985; Kolla and Perlmutter, 1993). Based on a geomorphological approach, Törnqvist et al. (2006) alternatively suggested that the glacial to LGM enhanced sediment flux to the deep-sea is unexpected on the French Atlantic margin (i.e. Armorican margin, Bay of Biscay) because the lowstand shoreline remained on the continental shelf (Figs. 1 and 2). Zaragosi et al. (2006) and

Fig. 2. Physiography of the northern French Atlantic margin (Western Approaches and Armorican margin, from North to South), with the present-day continent in green (ETOPO2 Global Relief Data), the continental shelf in white, and the continental slope and the abyssal plain (including the eastern part of the Celtic turbidite system and the Armorican turbidite system; e.g. Bourillet et al., 2006) in shades of grey (multibeam echosounder mosaic; Le Suavé et al., 2000). Between the coastline and the deep sea: the dashed blue line shows the course of the Fleuve Manche palaeoriver during lowstand intervals (Gibbard, 1988; Bourillet et al., 2003); the grey patches show the Neogene fluvial palaeovalleys (Reynaud et al., 1999; Menier et al., 2006; Le Roy et al., 2011); the dashed red line shows the coastal zone during the LGM (ca. 26.5–20 ka at global scale); the filled yellow areas show the SW–NE elongated Celtic sand banks (i.e. Western Approaches area; Reynaud et al., 2003); the green dashed line shows the topographic profile of Fig. 9; the solid red lines show the limits of the shelf break and of the continental slope (Bourillet et al., 2003); the yellow arrows depict the pathways of the turbidity currents (i.e. canyons and channels; Zaragosi et al., 2001b; Bourillet et al., 2003); the white areas show the location of the main sedimentary levees (Zaragosi et al., 2001b; Bourillet et al., 2003); the dashed yellow lines show the boundaries of the Celtic and Armorican turbidite systems (i.e. distal lobes; Zaragosi et al., 2001b; Bourillet et al., 2006). Core locations are shown by red and black circles, indicating turbiditic and hemipelagic environments, respectively; from west to east: MD95-2002 (Meriadzek Terrace), MD03-2690 (Guilcher levee), MD03-2688 (Crozon levee), MD03-2695 (Audierne levee) and MD03-2696 (Quiberon Ridge).

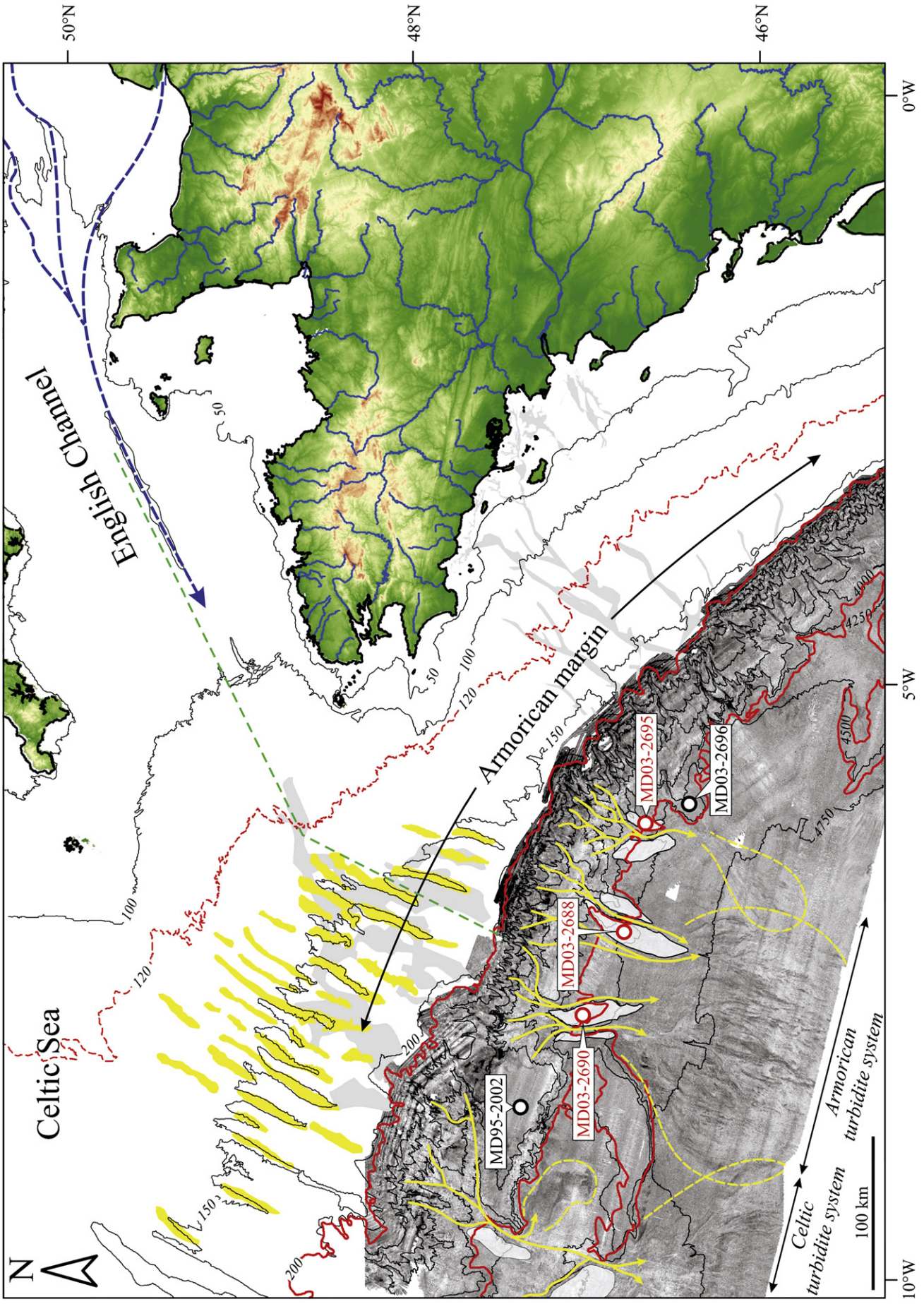
50°N
48°N
46°N
0°W
5°W
10°W
N
English Channel
Celtic Sea
Armorican margin
MD95-2002
MD03-2690
MD03-2688
MD03-2695
MD03-2696
50
100
120
150
200
4000
4250
4500
4750
Celtic turbidite system
Armorican turbidite system
100 km

Toucanne et al. (2008) partially challenged this hypothesis showing that there had been increasing turbidite supply to the Armorican turbidite system at the end of the last glacial period. The purpose of the present paper is to identify the response of the turbidite sedimentation and levee growth to river runoff and the shoreline migration on the Armorican shelf over the last 35,000 years, using new sedimentological data (turbidite grain-size, bed thickness) from three sedimentary levees.

2. Geological and palaeoenvironmental settings

2.1. The Armorican turbidite system

The Armorican turbidite system is a medium-sized turbidite system (~30,000 km^2) located in the central part of the Bay of Biscay (NE Atlantic, Figs. 1 and 2). It extends between 4100 and 4900 m water depth (mwd) at the foot of the low subsident Armorican margin (<25 m Ma^{-1}) (Zaragosi et al., 2001b; Bourillet et al., 2006). Connected to the southern part of the Celtic shelf (i.e. Western Approaches) and to the extensive Armorican shelf (~200 km wide and 360 km long) by about thirty deep canyons feeding three distinct channel–levee systems downstream (i.e. the Guilcher, Crozon and Audierne systems from west to east, Fig. 2), this system corresponds to a mud/sand-rich multiple-source ramp (Zaragosi et al., 2001b) according to the classification proposed by Reading and Richards (1994). Indeed, the Neogene fluvial palaeovalleys recognised from the Western Approaches to the Aquitaine shelf (Reynaud et al., 1999; Menier et al., 2006; Le Roy et al., 2011) suggest that the Armorican turbidite system was likely fed by many rivers during past sea-level lowstands, including the Fleuve Manche (Channel River) palaeoriver (Bourillet et al., 2003; Zaragosi et al., 2006; Toucanne et al., 2008). In addition, recent palaeotidal modelling suggests that the strong tidal pumping onto the Celtic and Armorican shelves, from which the giant linear tidal sand banks of the Celtic Sea originated (Berné et al., 1998; Reynaud et al., 2003; Scourse et al., 2009) (Fig. 1), likely contributed to the feeding of the Armorican turbidite system during transgressive and highstand conditions (Scourse et al., 2009).

The Guilcher, Crozon and Audierne systems show straight to low-sinuous channels (2 to 5 km wide, and 40 to 60 km long) and are bounded by strongly asymmetrical levees, the right levees being higher (i.e. channel–levee relief of ca. 100 to 170 m) and better developed (600 to 1100 km^2) than the left (Le Suavé et al., 2000; Zaragosi et al., 2001b) (Figs. 2 and 3). The distal part of the channel network corresponds to lobe deposits, which have been described as stacked small-scale finger-like sublobes (Zaragosi et al., 2001b) (Fig. 2). Sub-bottom profiling records (Chirp, 3.5 kHz) over these systems show acoustically well-developed, stratified overbank deposits with sharp, smooth and continuous sub-bottom reflectors corresponding to muddy spillover deposits (Fig. 3). This process has been corroborated by the detailed study of long-piston cores showing some fining-upward millimetre- to centimetre-scale silt to sand deposits with erosional base and internal sedimentary structures (Zaragosi et al., 2001b, 2006; Toucanne et al., 2008) interpreted as T*cde* turbidites resulting from turbidity flows (Stow and Piper, 1984). Conversely, the prolonged echo that characterises the channel and lobe deposits suggests that they consist of coarse-grained sediments (Zaragosi et al., 2001b) (Fig. 3). Seismic data reveal that the studied channel–levee systems slowly migrated eastward (<400 m Ma^{-1} in the middle ramp since the Early Miocene; Mansor, 2004) in a net aggradational setting (see Fig. 3 for the Late Quaternary).

Seismic data suggest that fan deposition began during the Early Miocene. The depositional system then progressively extended towards the deep basin during the Plio–Quaternary in response to increasing sediment supply from the NW European margin (Droz et al., 1999; Mansor, 2004). The Quaternary glaciations in Europe strongly increased the sediment supply to the deep sea through fast-moving ice streams and ice-sheet derived meltwater flows, especially since the mid-Pleistocene transition (MPT, from ca. 1250 to 700 ka) (Sejrup et al., 2005; Toucanne et al., 2009b; Laberg et al., 2011). A strong relationship between the oscillations of the European ice-sheet and the evolution of the Armorican turbidite system has been demonstrated for the Late Quaternary (Zaragosi et al., 2000, 2001a, 2006; Toucanne et al., 2008, 2010). The Armorican margin thus represents a passive margin depositional system, transitional between the true glacial ice stream–trough mouth fan systems to the north (i.e. glaciated margins north of 56°N) and the fluvial canyon systems characteristic of the Aquitaine margin (between 44°N and 46°N) to the south (Scourse et al., 2009).

2.2. Sediment sources: the European ice-sheets and the Fleuve Manche palaeoriver

The Pleistocene was a period of fluctuating climate accompanied by prominent sea-level lowstands during the glacial intervals, when massive continental ice sheets extended from mountainous to lowland areas over Europe, as far as about 50°N (Ehlers et al., 2011) (Fig. 1). The seaward retreat of the shoreline on the extensive shallow continental shelves of the southern and eastern parts of the British Isles induced a reorganisation of the European drainage network and the appearance of large rivers, with considerable drainage catchments, after the merging of present-day French and British rivers and German and Dutch rivers on the subaerially exposed English Channel and North Sea basin, respectively (Gibbard, 1988) (Fig. 1). Complex networks of palaeovalleys reveal that the present-day Somme, Seine, Solent and numerous minor French and British rivers merged into the English Channel to form the Fleuve Manche palaeoriver (Gibbard, 1988; Lericolais et al., 1996, 2003; Bourillet et al., 2003). During the last glacial period (71–14 ka BP), the Fennoscandian (FIS) and British–Irish (BIIS) ice-sheets reached a maximal extension between ca. 30 and 20 ka (i.e. during the global Last Glacial Maximum, LGM, 26.5–20 ka according to Clark et al., 2009) (Clark et al., in press). Their coalescence in the intervening North Sea induced a strong modification of the fluvial directions of the central European rivers, thus forcing the present-day Vistula, Oder, Elbe, Rhine and Thames rivers to flow to the English Channel (Toucanne et al., 2010) (Fig. 1). The deep-sea sedimentation in the northern Bay of Biscay was strongly influenced by the Fleuve Manche palaeoriver discharges throughout the last glacial period, and its last large-magnitude palaeoflow event – from ca. 20 ka, with a maximum intensity between ca. 18.3 and 17 ka – occurred at the onset of Termination I, in phase with the rapid retreat of the mid-latitudinal European ice sheets and glaciers (Zaragosi et al., 2001a; Ménot et al., 2006; Eynaud et al., 2007; Toucanne et al., 2009a, 2010).

3. Material and methods

This study is based on Calypso long-piston cores retrieved from the crest of the Guilcher (site MD03-2690; 47°01.25′N, 07°44.99′W; 4340 mwd), Crozon (site MD03-2688; 46°48.03′N, 07°02.93′W; 4385 mwd) and Audierne (site MD03-2695; 47°43,14′N, 06°12,68′W; 4375 mwd) levees (from west to east, Figs. 1 to 3) during the MD133-SEDICAR oceanographic cruise onboard the R/V *Marion Dufresne II* (IPEV). Details about cores and coring sites are given in Figs. 1 to 3.

3.1. Chronostratigraphic framework

The chronostratigraphic framework of cores MD03-2690, MD03-2688 and MD03-2695 was based on 28 AMS ^{14}C dates (French Project ARTEMIS ^{14}C AMS) complemented by an analysis of the relative abundance of *Neogloboquadrina pachyderma* (sinistral coiling) and

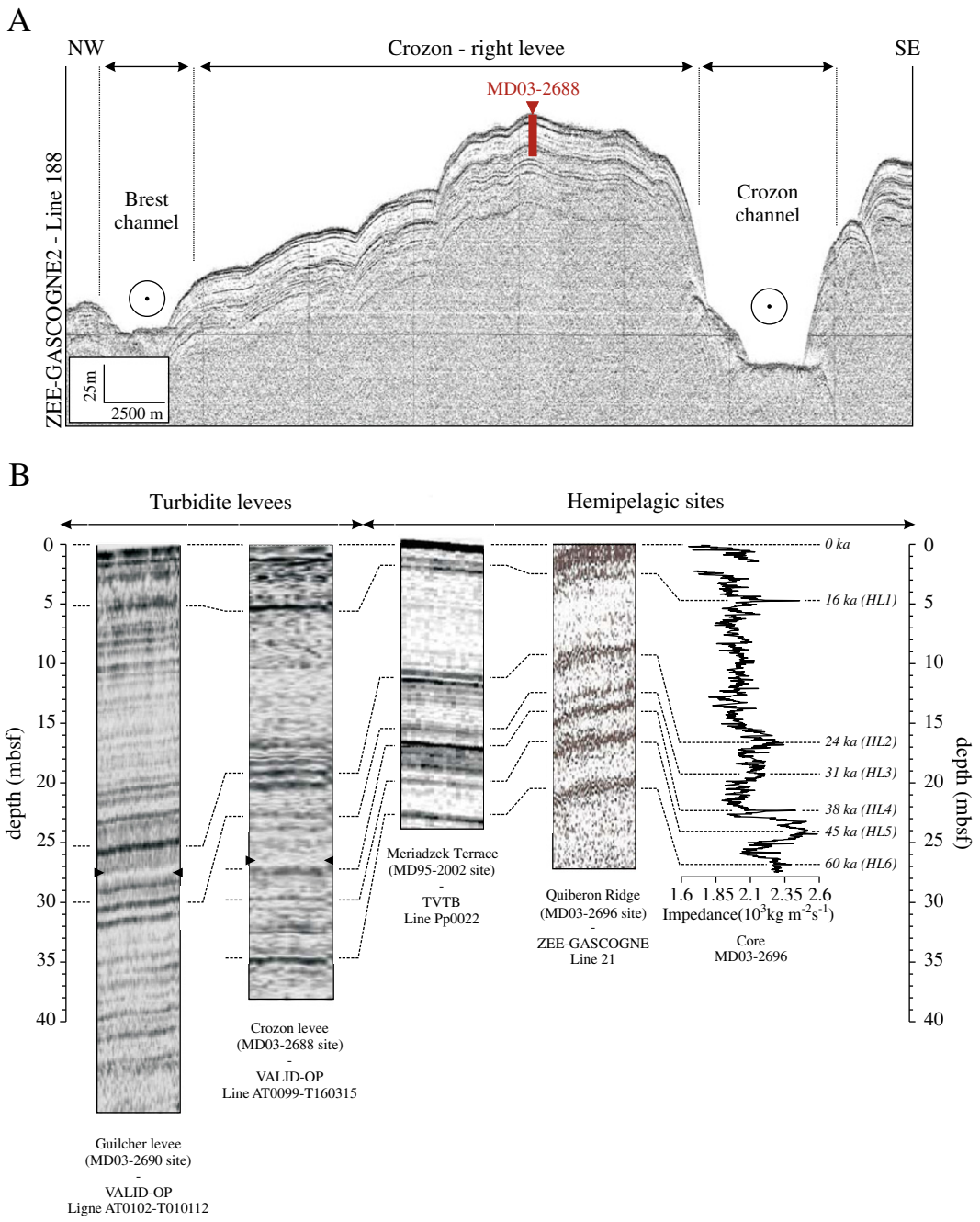

Fig. 3. (A) 3.5 kHz acoustic profile of the Crozon channel–levee system and location of core MD03-2688 (in red on the levee crest). The acoustic dataset demonstrates a net aggradation of the levee crest and this process dominates for the time period sampled in core MD03-2688. See Fig. 2 for location of core MD03-2688; (B) Site-to-site correlations of acoustic data (3.5 kHz, Chirp) from turbiditic and hemipelagic depositional environments of the Armorican margin. Correlations of acoustic data with impedance contrasts (i.e. velocity times density) of in-situ well-dated sediment cores permitted the main acoustic horizons to be interpreted as the Heinrich layers (HL), as demonstrated for the Quiberon Ridge with core MD03-2696 (Toucanne et al., 2010). The significant difference between the depth of high impedance layers in the Quiberon Ridge (i.e. acoustic horizons on 3.5 kHz data) and within core MD03-2696 indicates that stretching occurred in the upper part of the core (i.e. coring artefact). The black triangles on the acoustic data at sites MD03-2688 and MD03-2690 indicate the bottom of the cores.

ice-rafted debris (IRD) counting from hemipelagic layers (Zaragosi et al., 2006; Toucanne et al., 2008) (Fig. 4). *N. pachyderma* (s) and IRD in the Bay of Biscay identify abrupt sea-surface changes and glacial-rainout intervals which are stratigraphically contemporaneous with major climatic events (i.e. Heinrich stadials and Dansgaard–Oeschger oscillations) (Grousset et al., 2000). Age models were constructed using radiocarbon dates and additional control points from cores MD03-2696 (Quiberon Ridge; 46°29.51′N, 06°02.36′W; 4422 mwd) and MD95-2002 (Meriadzek Terrace; 47°27.12′N, 08°32.03′W; 2174 mwd) (Fig. 4), both located in hemipelagic depositional environments (Fig. 2). The age model of core MD95-2002 is based on 20 ^{14}C AMS ages spanning the last 30 ka (Grousset et al., 2000; Zaragosi et al., 2006) (Fig. 4). It should be noted that the average age and duration of the Heinrich stadials recognised in the Bay of Biscay are consistent with those widely accepted in the recent literature (Barker et al., 2009; Denton et al., 2010). The detailed methodology is given in Zaragosi et al. (2006) and Toucanne et al. (2008).

3.2. Sedimentological analyses

The sedimentological analyses of cores MD03-2690, MD03-2688 and MD03-2695 consisted firstly of visual description and X-ray

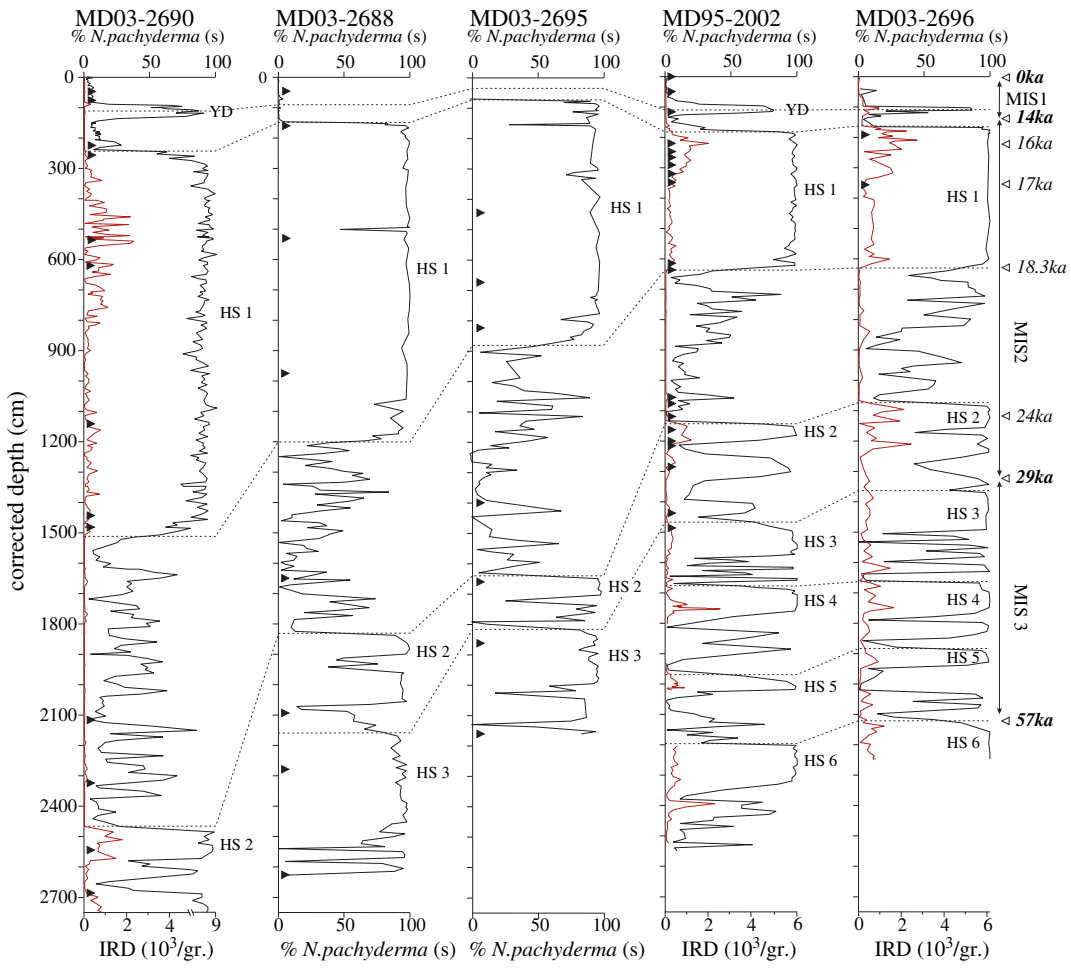

Fig. 4. Abundance of planktic foraminifers *Neogloboquadrina pachyderma* (s) (continuous black line — %) and of IRD (red line — 10^3/g) from sediment cores MD03-2690, MD03-2688 and MD03-2695 (turbidite levees), MD95-2002 and MD03-2696 (hemipelagic depositional environments). Dashed black lines represent core-to-core correlations using the Younger Dryas interval (YD), the upper limit of Heinrich stadials (HS) 2 to 6 and the lower and upper limits of the HS 1. AMS ^{14}C dated samples are marked by black triangles on the depth scale. Ages are shown in bold type and associated open triangles delimit the Marine Isotope Stages (MIS) boundaries according to Lisiecki and Raymo (2005). Intermediate ages and associated open triangles within the MIS 2 refer to the ages used in the Discussion.

analyses (SCOPIX imaging system), which allowed the recognition of turbidite deposits. Grain size at the base of the thickest turbidites (~15–20% of the total number of turbidites counted in cores MD03-2690, MD03-2688 and MD03-2695, i.e. 365 analysis) was analysed using a Malvern™ Supersizer 'S'. In addition, we estimated the thickness of each turbidite recognised in cores MD03-2690, MD03-2688 and MD03-2695. The detailed examination of the sediment using X-ray imagery revealed that stretching prevails in the upper part of the cores, due to cable rebound causing upward piston acceleration (Skinner and McCave, 2003; Bourillet et al., 2007). As a result, turbidite thickness, as well as sediment accumulation rates, were estimated once correction of these coring artefacts had been made. This correction was realised using the CINEMA software (Bourillet et al., 2007) in combination with the correlations of impedance contrasts (i.e. velocity times density, measured using a Geotek Multi Sensor Core Logger) of the well-dated cores with very high-resolution acoustic data (see Toucanne et al. (2010) for details) (Fig. 3). Defining the top of a turbidite sequence (by using X-ray imagery or grain-size analyses, for instance) can be difficult, introducing some uncertainty about turbidite thickness measurements (Sadler, 1982; Stow and Piper, 1984). Here, the turbidite thickness was calculated from turbidite base to turbidite base because (*i*) the boundaries between the upper part of the turbidites and the above hemipelagic layers are indistinguishable on X-ray images, (*ii*) the number of turbidites in each core is too many to discriminate turbidite and hemipelagic deposits using grain-size analyses (up to 920 turbidites in cores MD03-2690) and (*iii*) most of the facies show stacked turbidite deposits (e.g. ultra-laminated facies). Associated with the high-resolution chronostratigraphic framework and the age model of the cores, the counting of the turbidites (total of ca. 2300) has allowed the calculation of the turbidite deposit frequency (with a 250 year-period, i.e. the number of turbidite beds per time slice of 250 years) on the Guilcher, Crozon and Audierne levees. We consider this quantification to represent the minimum value of turbidite frequency, because of possible erosive losses and/or non-deposit events (i.e. by-pass).

4. Results

4.1. Sedimentary facies

The detailed sedimentological analyses (visual description, X-ray imagery, grain-size measurements and thin-section analysis) of the studied cores, associated with the analysis of foraminifera assemblages, allowed the identification of six facies (Fig. 5A and Table 1). Facies 1 consists of light beige, homogeneous, structureless

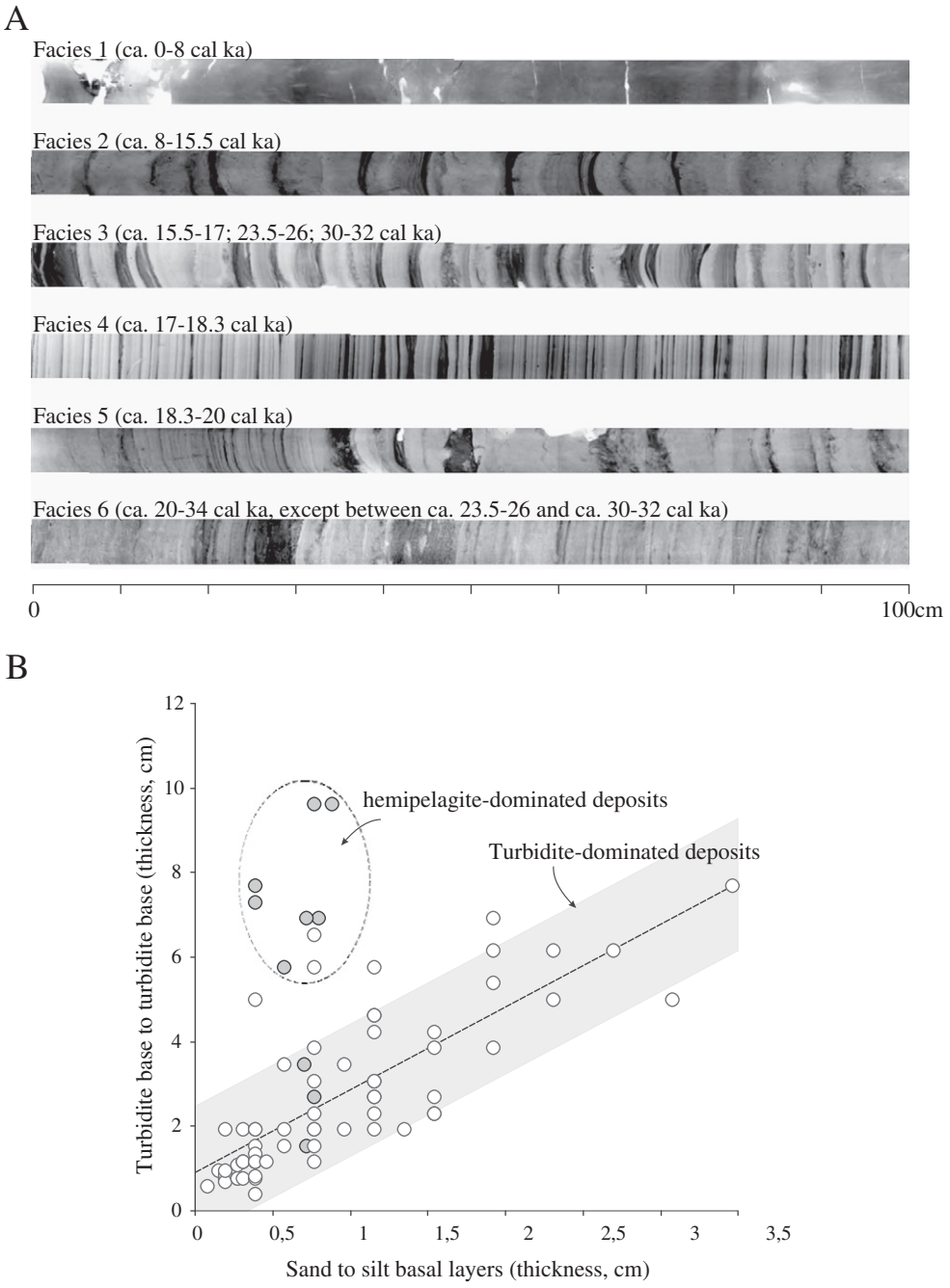

Fig. 5. (A) Examples of some representative X-rayed slabs of facies 1 to 6 are described by Toucanne et al. (2008), illustrating the evolution of the turbidite facies in the Armorican channel–levee systems throughout the last 35 ka. (B) Detailed analysis of the above X-rayed slabs, i.e. the relationship between the thickness of the sand to silt basal turbidite layers (i.e. the dark layers on the X-ray images) and the thickness of the deposits from turbidite base to turbidite base (i.e. extended turbidites, including the hemipelagic layers). Grey circles: analyses of the deposits of facies 2; white circles: analyses of the deposits of facies 1 and facies 3 to 6. The positive correlation existing between the thickness of the turbidite basal layers and the thickness of the extended turbidites (i.e. including the hemipelagic layer) reveals that only the extended turbidites deposited after ca. 15 ka (i.e. facies 2) cannot be considered as turbidite-dominated deposits (i.e. turbidites sensu stricto).

foraminifera-rich silty-clay (30–50% biogenic $CaCO_3$), with abundant bioturbation and containing a temperate foraminiferal assemblage typical of the Holocene period in the region (*Globigerinoides ruber*, *Globigerina bulloides*, *Globorotalia hirsuta*, *Globorotalia truncatulinoides*, etc.). This facies, recognised in the upper part of cores MD03-2690, MD03-2688 and MD03-2695, is similar to that found at the top of cores MD95-2002 and MD03-2696, which are located in hemipelagic depositional environments (Zaragosi et al., 2001a; Auffret et al., 2002) (Fig. 2). Facies 1 was deposited between 0 and ca. 8 ka (Toucanne et al., 2008). Facies 2 to 6, deposited between 8 and 35 ka, consist of silt or sand deposits embedded in a brownish homogeneous silty-clay (10–20% biogenic $CaCO_3$) containing temperate to polar–subpolar foraminiferal assemblages typical of the last glacial period in the Bay of Biscay (*G. bulloides*, *Globigerina quinqueloba* and *Neogloboquadrina pachyderma*, dextral and sinistral coiling). The presence of IRD, especially in facies 3 and 4 in which a monospecifism of the polar foraminifera *N. pachyderma* (s) is observed, corroborates this biostratigraphic interpretation. The silt or sand deposits show sharp or erosional basal contacts and are normally graded. Internal structures such as horizontal laminations and ripple cross-

Table 1
Summary of sedimentary facies characteristics. X-ray images of facies 1 to 6 are shown in Fig. 5A.

Facies	Age (ka)	Sedimentological description	Turbidite base grain size (μm)	Turbidite freq. (turb.250 yr^{-1})	SAR (cm.kyr^{-1})	Interpretation/Origin
1	0–8	Homogeneous, structureless marly ooze	No turbidite	No turbidite	≤10	Hemipelagic deposits
2	8–15.5	Homogeneous clay interbedded with some cm-scale silt to very fine sand layers	50–110	≤10	≤150	Fine-grained turbidites deposited from the overflow of turbidity currents
3	15.5–17 23.5–26 30–32	Frequent thinning- and fining-upward sequences of silt and very fine to fine sand deposits with erosive basal contacts	50–200	10–30	100–500	Fine-grained turbidites deposited from the overflow of turbidity currents
4	17–18.3	Ultra-laminated sediment showing mm-scale fining-upward silty laminae and rare silty to very fine sandy deposits	20–90	40–70	500–700	Very fine-grained turbidites (deposited by hyperpycnal meltwater flows?)
5	18.3–20	Homogeneous clay interbedded with numerous fining-upward mm- to cm-scale silt to fine sand deposits with erosive basal	50–150	20–40	250–400	Fine-grained turbidites deposited from the overflow of turbidity currents
6	20–23.5 26–30 32–35	Massive, fining-upward silt to sand deposits embedded in a homogeneous clay	50–200	≤10	≤150	Fine-grained turbidites deposited from the overflow of turbidity currents

stratifications are observed (e.g. facies 3 and 6). The silt or sand deposits vary in thickness from a few millimetres in facies 4 (ultra-laminated facies showing numerous fine fining-upward silty laminae with sharp basal contacts deposited during the European deglaciation, 18.3–17 ka; Zaragosi et al., 2006; Toucanne et al., 2008) up to 18 cm in facies 6 (rare, massive, fining-upward coarse silt to fine sand deposits with erosional basal contacts). Both this latter facies and facies 3 (frequent thinning- and fining-upward sequences of coarse silt and very fine sand deposits with erosional basal contacts) are characteristic of full glacial conditions (LGM and Late glacial), while facies 5 and 2 are characteristic of transitional periods in the sedimentation, from full glacial (LGM, facies 6) to deglacial conditions (in Europe, ca. 18.3–17 ka, facies 4) and from Late glacial (at global scale, ca. 17–15.5 ka, facies 3) to interglacial conditions (8–0 ka, facies 1), respectively (Fig. 5A). According to the classification of Stow and Piper (1984), we interpreted the silt and sand beds as representing fine-grained turbidites deposited from the overflow of turbidity currents (spillover deposits from surge-like turbidity currents), while we interpreted homogeneous silty-clay as hemipelagic deposits (see Toucanne et al., 2008 for details). Turbidite activity is detailed thereafter through the calculation of turbidite frequency, while turbidite thickness and turbidite grain-size allowed the investigation of the processes by which turbidity currents are initiated, and potential changes in the sediment source (Sadler, 1982; Manley et al., 1997; Talling, 2001).

4.2. Turbidite frequency and accumulation rates

Turbidite frequency was estimated from cores MD03-2690, MD03-2688 and MD03-2695 over 250-year interval steps (Fig. 6). The results show remarkably similar values and evolution of turbidite frequency in the three levees. Three main periods of turbidite activity are observed:

(i) From 34 to 20 ka, the Guilcher, Crozon and Audierne channel–levee systems are characterised by a generally low turbidite frequency, ranging from 0 to 15 turbidites per 250 years. A moderate turbidite frequency was observed between 32 and 30 ka (i.e. Heinrich stadial 3), and between 26 and 23.5 ka (i.e. Heinrich stadial 2) (10 to 15 turbidites per 250 years) while the intervening periods had very low turbidite frequency (0 to 5 turbidites per 250 years). The sediment accumulation rates (i.e. levee growth) ranged from 30 to 60 cm ka^{-1} during the 35–24 ka interval, and reached up to 100 cm ka^{-1} at the MD03-2690 site between 24 and 20 ka.

(ii) Between 20 and 17 ka, there was a major increase in the turbidite frequency (up to ca. 70 turbidites per 250 years in the three studied cores). A first increase in the turbidite frequency was observed between 20 and 19 ka, followed by a second increase of higher amplitude between 18.3 and 17 ka. The sediment accumulation rates ranged from 500 to 700 cm ka^{-1} during the latter interval. A sharp decrease of turbidite frequency occurred between 17 and 16 ka (ca. 15 turbidites per 250 years around 16 ka).

(iii) From 16 to 14 ka, there was a gradual decrease of turbidite frequency from around 15 turbidites per 250 years around 16 ka to a maximum of 5 turbidites per 250 years around 14 ka. The sediment accumulation rates reached only ca 20–50 cm ka^{-1} after 16 ka. The turbidite frequency ranged from 0 to 3 turbidites per 250 years between 14 and 9 ka, and no turbidites could be found at sites MD03-2690, MD03-2688 and MD03-2695 for the period after 8 ka.

4.3. Turbidite thickness

Turbidite thickness was calculated in cores MD03-2690, MD03-2688 and MD03-2695 (Fig. 7). A positive correlation between the thickness of the turbidites (i.e. possibly including a hemipelagic layer, see Section 3.2) and the thickness of the silt to sand basal layers (i.e. dark layers on the X-ray images, Fig. 5A) was observed (Fig. 5B). Previous studies in which turbidites were easily distinguished from hemipelagic deposits show that turbidite bed thickness and sand-interval thickness are positively correlated (Sadler, 1982; Talling, 2001). As a result, the positive correlation described above for cores MD03-2690, MD03-2688 and MD03-2695 likely suggests that the turbidites recognised in the Guilcher, Crozon and Audierne levees are embedded between thin hemipelagic deposits (except in the upper part of the cores, see below).

Turbidite thickness shows a very similar evolution in the three levees (Fig. 7). Due to the significant relationships existing between turbidite frequency and turbidite thickness (i.e. negative correlation, Fig.7), the results for turbidite thickness are presented using the time periods previously used for the evolution of the turbidite frequency:

(i) From 34 to 20 ka, turbidite thickness exhibited a significant variability ranging from 1 to 18 cm (with silt to sand basal layers up to 7–9 cm thickness), with maxima of ca. 10–18 cm during the 34–32 ka and 23.5–20 ka intervals (i.e. facies 6, Fig. 5A), and minima of ca. 1–6 cm between 32 and 30 ka (i.e.

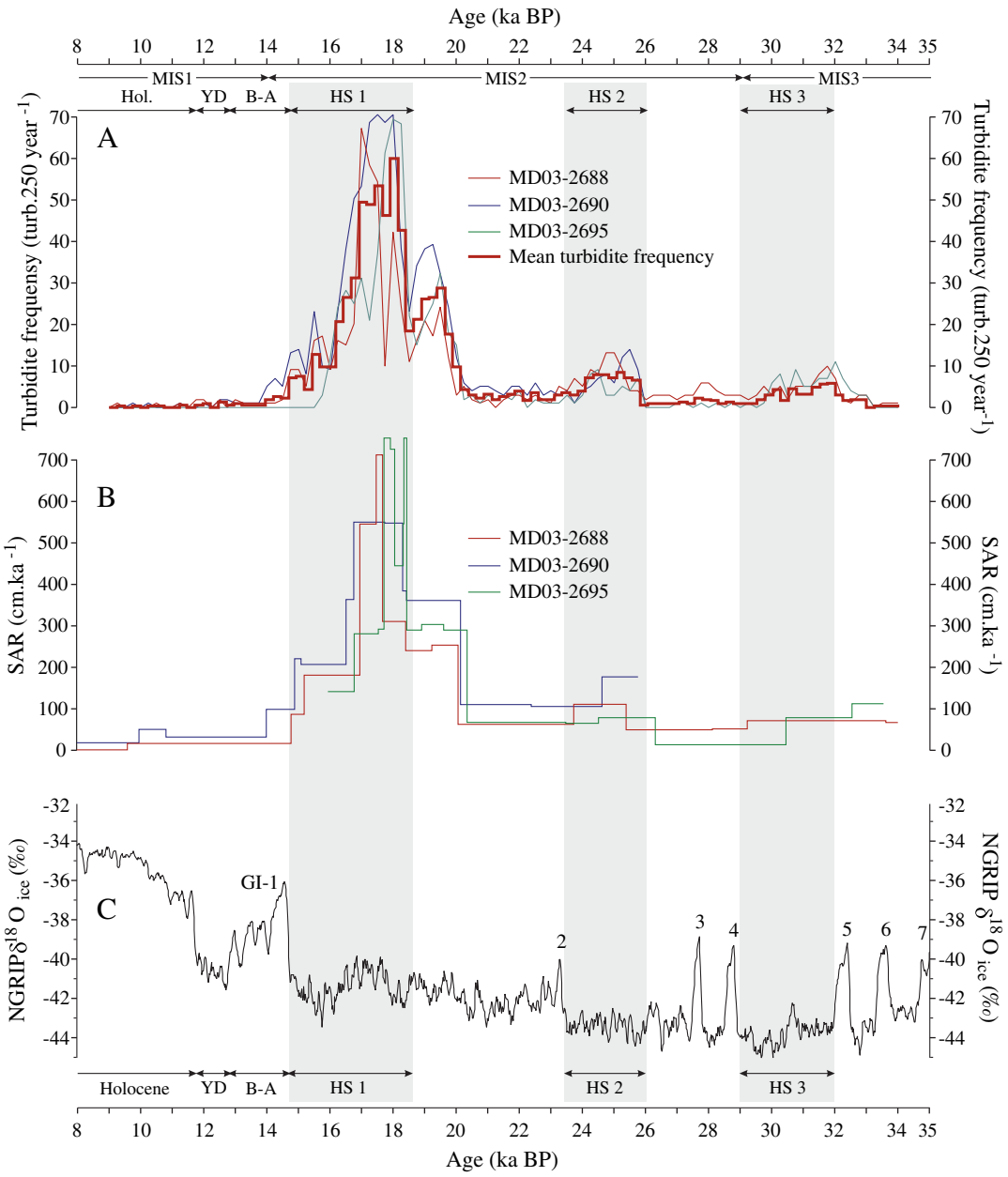

Fig. 6. (A) Turbidite frequency (with a 250-year resolution) for cores MD03-2690, MD03-2688 and MD03-2695 between 8 and 35 ka; (B) Sediment accumulation rates (SAR, cm ka^{-1}) at sites MD03-2690, MD03-2688 and MD03-2695 are according to the chronology detailed in Fig. 4 and in Toucanne et al. (2008). (C) The NorthGRIP $\delta^{18}O$ profile (GICC05 chronology; Svensson et al., 2008). The Greenland Interstadials are indicated as GI. Marine Isotope Stages (MIS) boundaries according to Lisiecki and Raymo (2005). B–A: Bölling–Alleröd, YD: Younger Dryas. Light grey bands indicate the Heinrich stadials (HS).

Heinrich stadial 3) and between 26 and 23.5 ka (i.e. Heinrich stadial 2) (i.e. facies 3, Fig. 5A). An intermediate mean thickness of ca. 5–10 cm was observed between 30 and 26 ka.

(ii) Between 20 and 17 ka, the mean turbidite thickness was significantly lower than during the 34–20 ka interval. In detail, a significant decrease of the turbidite thickness occurred from ca. 24–21 ka (10–15 cm) to ca. 20–19 ka (5 cm max., but usually <3–4 cm) (i.e. facies 5, Fig. 5A). The minimal turbidite thickness was observed during the 20–19 ka and 18.3–17 ka intervals (1–2 cm thickness max., with millimetre-scale basal layers; i.e. facies 4, Fig. 5A). A slight increase (5–10 cm) was observed at around 18.5 ka.

(iii) From 16 to 9 ka, the turbidite thickness increased, with values usually above 3–5 cm (i.e. facies 3, Fig. 5A) and up to ca. 15–20 cm in the upper part of the interval (i.e. facies 2, Fig. 5A). From ca. 15 ka, the estimation of the turbidite thickness from turbidite bases becomes unreliable. Although the silt to sand basal layers remained constant (ca. 1 cm thickness), the thickness of the studied deposits increased significantly. We assume that the decrease of the turbidite frequency during this interval allowed more time for accumulation of terrigenous and biogenic material from vertical settling and slow lateral advection (i.e. hemipelagite), the studied deposits thus represent hemipelagite-dominated deposits rather than turbidite-dominated deposits (Fig. 5B).

4.4. Turbidite grain size

The grain size of the silt to sand base of 103 to 137 turbidites was analysed in each core (Fig. 7). Despite significant variability, the results showed very similar values and evolution in the three levees.

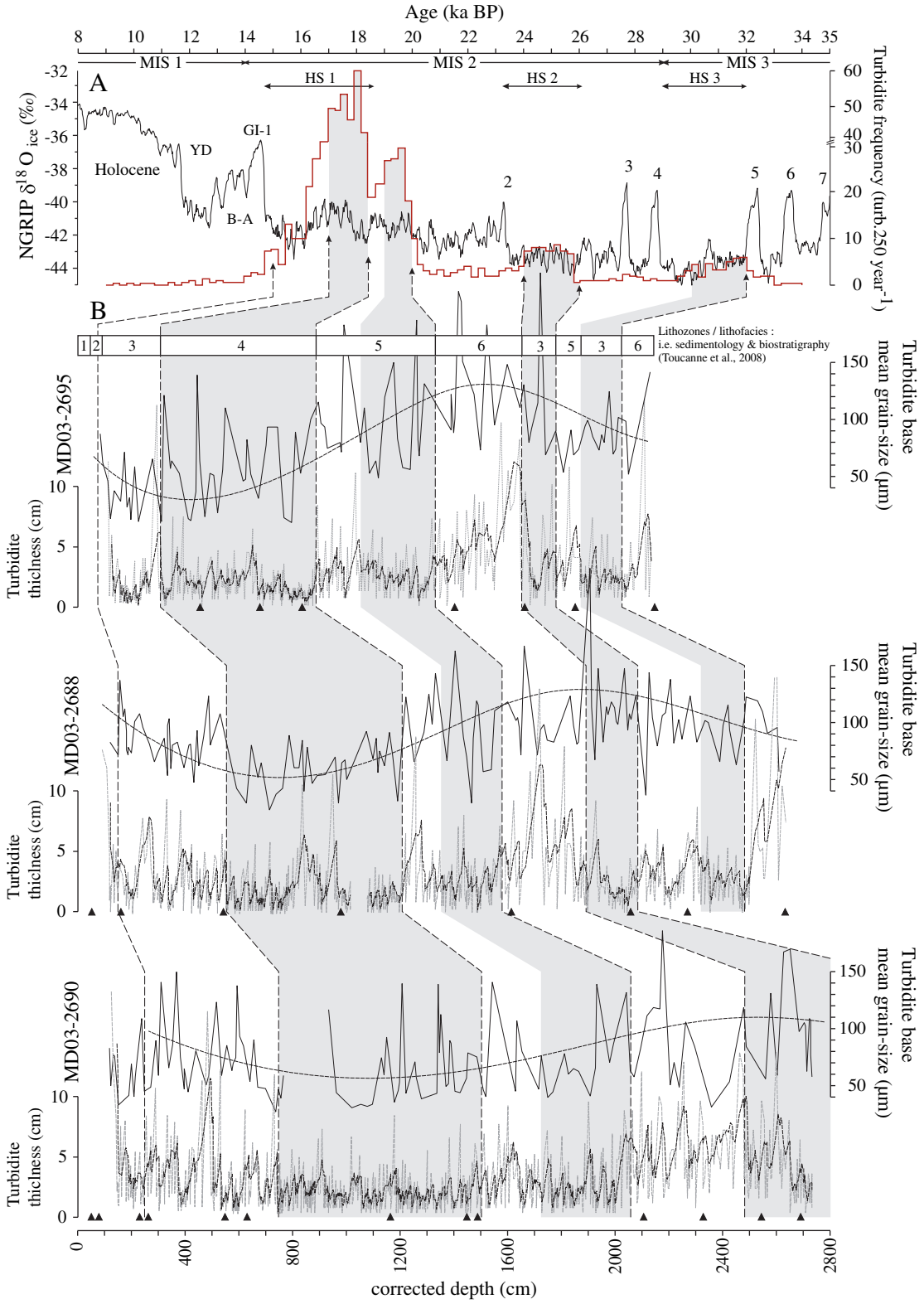

Fig. 7. (A) Mean turbidite frequency (250-year resolution) for cores MD03-2690, MD03-2688 and MD03-2695 (red line; see Fig. 6 for details) and the NorthGRIP $\delta^{18}O$ profile (black line) (GICC05 chronology; Svensson et al., 2008). The Greenland Interstadials are as indicated GI. (B) Turbidite thickness (dashed grey lines — cm; three-points moving average shown as dashed black lines) and mean grain-size of turbidite bases (continuous black lines — µm; fifth-order polynomial average shown as dashed black lines) in cores MD03-2690, MD03-2688 and MD03-2695. Vertical dashed lines represent core-to-core correlations. Grey shaded zones show the periods of increasing turbidite frequency. Facies 1 to 6 refer to Fig. 5A and Table 1 (Toucanne et al., 2008). Marine Isotope Stages (MIS) boundaries according to Lisiecki and Raymo (2005). B–A: Bölling–Alleröd, YD: Younger Dryas, LGM: Last Glacial Maximum, HS: Heinrich stadials.

Three main periods in the evolution of the mean grain size of the turbidites are observed in the Guilcher, Crozon and Audierne levees:

(i) From 34 to 26–24 ka, the mean grain size of the turbidite bases gradually increased from ca. 60–100 μm to ca. 100–150 μm in cores MD03-2688 and MD03-2695.
(ii) Between 26–24 and 18–17 ka, the mean grain size of the turbidite bases gradually decreased, to reach minimum mean values of around 20–60 μm at ca. 17.5 ka in cores MD03-2688 and MD03-2695. The lower values ranged from 30 to 40 μm in core MD03-2690 around this period, while ranging from 40 to 70 μm at ca. 24–22 ka.
(iii) Between 18–17 and 15–14 ka, a significant increase of the mean grain size was observed for the turbidite bases, especially in cores MD03-2688 and MD03-2690, in which the increase reached about 30–40 μm in amplitude over this period.

5. Discussion

5.1. Evolution of turbidite sedimentation onto the Guilcher, Crozon and Audierne levees over the last 35 ka

Sedimentological profiles from the deep-sea sediment cores MD03-2690, MD03-2688 and MD03-2695, coupled with a robust chronological framework, provide a high-resolution record of the sedimentation onto the Guilcher, Crozon and Audierne levees over the last 35 ka. Our dataset reveals that significant turbidite activity with spillover processes controlled the levee growth in the Guilcher, Crozon and Audierne channel–levee systems during the last glacial period, from 35 ka until 8 ka, while only slow accumulation of terrigeneous and biogenic material have occurred since 8 ka (Figs. 5 and 6).

Turbidite flux (i.e. sediment accumulation rates and turbidite frequency) onto sedimentary levees and turbidite texture (i.e. thickness and grain-size) depend on the nature, volume and competence of the turbidity currents, with all these parameters controlling the ability of the turbidity currents to spill out of the confining channels (Skene et al., 2002; Dennielou et al., 2006; Straub and Mohrig, 2008). Recent studies show that (frequent) small turbidity currents die out in the channel, and hence that only (rare) large turbidity currents are able to overspill the levees (e.g. Khripounoff et al., 2009; Mas et al., 2010; Jorry et al., 2011 for the Var deep-sea fan). Nakajima and Itaki (2007) discussed this process and assumed, in agreement with these observations, that the increase in turbidite frequency, turbidite thickness and grain-size results from increased sediment delivery to the channel system. Levee deposits are, therefore, suitable for describing the entire turbidite-system growth. The consistency of our results obtained from three channel–levee systems connected to distinct canyon networks (Fig. 2), supports this latter hypothesis.

The high-resolution reconstruction of the sediment accumulation rates and turbidite frequency shows that the amount of turbidite accumulation on the Guilcher, Crozon and Audierne levees was concomitant (Fig. 6). This suggests that the sediment supply of the three feeding canyon networks was controlled by a common forcing. In detail, the sediment flux on the levees was low from 35 to 20 ka (maximum of 15 turbidites per 250 years; sediment accumulation rates of ca. 100 cm ka^{-1}). It increased significantly from ca. 20 ka, i.e. at the onset of Termination I, then reached a maximum between ca. 18.3 and 17 ka (up to 70 turbidites per 250 years; sediment accumulation rates ranging from 500 to 700 cm ka^{-1}). The sediment flux rapidly decreased thereafter (maximum of 15 turbidites per 250 years at 16 ka; sediment accumulation rates of <50 cm ka^{-1}) and no turbidite sedimentation occurred after ca. 8 ka. Interestingly, sediment fluxes fluctuated in phase with major climate oscillations (e.g. LGM, Early deglaciation, and Holocene). This suggests that the sediment fluxes into the Armorican turbidite system were likely controlled by external forcing, particularly climate oscillations and associated palaeoenvironmental changes (e.g. sea-level changes, fluvial discharges, etc.). This relationship between climate and turbidite sedimentation in the Armorican turbidite system is emphasised at the onset of Termination I, between ca. 20 and 17 ka. The increased sediment delivery at that time coincided with the retreat of the mid-latitudinal ice sheet in Europe (Rinterknecht et al., 2006) and the onset of eustatic sea-level rise (Clark et al., 2009) (Figs. 8 and 9), thus making the Armorican turbidite system a transgression-dominated system sensu Covault and Graham (2010). Moderate pulses of sediment delivery at Heinrich stadials 3 and 2 also suggest that climate forcing controlled the turbidite sedimentation during the last glacial period (Figs. 6, 7 and 8).

Similarly, significant changes in grain size and turbidite thickness occurred concomitantly on the Guilcher, Crozon and Audierne levees over the 35–8 ka period. In detail, two phases of increasing turbidite thickness and basal grain size occurred in the early LGM (ca. 35–24 ka) and after ca. 17 ka, bracketing a significant decrease in both parameters from ca. 24 ka to ca. 18–17 ka (Figs. 7 and 8). Such a turbidite deposition pattern is unexpected for levee morphology evolution under aggradational conditions (net aggradation of about 20–30 m over the period; Fig. 3). Indeed, levee aggradation would gradually increase the confinement of the turbidity currents within the channel, decreasing the likelihood of the spillover of subsequent turbidity currents (Skene et al., 2002; Straub and Mohrig, 2008). As a result, a fining upward trend of the thickness and grain size of the overspill deposits is commonly observed (Hiscott et al., 1997; Manley et al., 1997; Dennielou et al., 2006). This suggests that the fluctuations of the grain size and thickness of the turbidites described at sites MD03-2690, MD03-2688 and MD03-2695 were controlled by fluctuations in the composition and provenance of the sediments, and also in the trigger mechanisms of the turbidity currents. The concomitance of the fluctuations on the three levees and the phase relationship with climatic changes show that composition, provenance and trigger mechanism were controlled by climate-driven external forcings, which were likely to have been sea-level and river-runoff fluctuations.

5.2. Unravelling external forcing effects on sedimentation and levee growth

Detailed analysis of the Guilcher, Crozon and Audierne levees reveals that climate forcing has controlled the turbidite sedimentation in the Armorican turbidite system over the last 35 ka (Fig. 8). Climate oscillations in western Europe during the last glacial period, in addition to glacio-eustatic sea-level fluctuations which controlled the drainage basin morphology and the river–canyon connection (Mulder and Syvitski, 1996), probably led to significant changes in sediment delivery to the Bay of Biscay and thus in the evolution of the Armorican turbidite system.

5.2.1. The glacial period (35–20 ka)

Sequence stratigraphic models predict that turbidite sedimentation strengthened during sea-level fall and reached a maximum during sea-level lowstand, with fluvial systems delivering their sedimentary loads directly to the heads of submarine canyon–channel systems (Stow et al., 1985; Posamentier and Vail, 1988; Covault and Graham, 2010). During the last glacial period, the sea-level gradually fell from −40/−80 m to −120 m between ca. 35 and 26.5 ka, and maximal lowstand conditions (ca. −120 m) prevailed throughout the global LGM, ca. 26.5 to 20 ka (Siddall et al., 2008; Clark et al., 2009). Surprisingly, our results reveal low sediment flux in the Armorican turbidite system during this interval (Figs. 6, 8 and 9). Levee growth ranged from only 30 to 100 cm ka^{-1} during the LGM, the turbidite frequency was also weak, with only ca. 5 events per 250 years between 24 and 20 ka, and sedimentation was characterised by sandy turbidites (i.e. facies 6, Fig. 5A). As a result, we conclude that only rare sand-rich density flows fed the Armorican turbidite system

during the LGM lowstand. The low sediment delivery to levees probably reflects the weak discharge of the Fleuve Manche due to the prevailing contemporaneous arid conditions on the surrounding local land, and because the ice sheet failed to release substantial meltwater volumes during the last glacial period (Ménot et al., 2006; Toucanne et al., 2010) (Fig. 8). The shelf physiography would definitely also have caused low sediment delivery (Törnqvist et al., 2006). The present-day bathymetry of the shelf-break is ca.

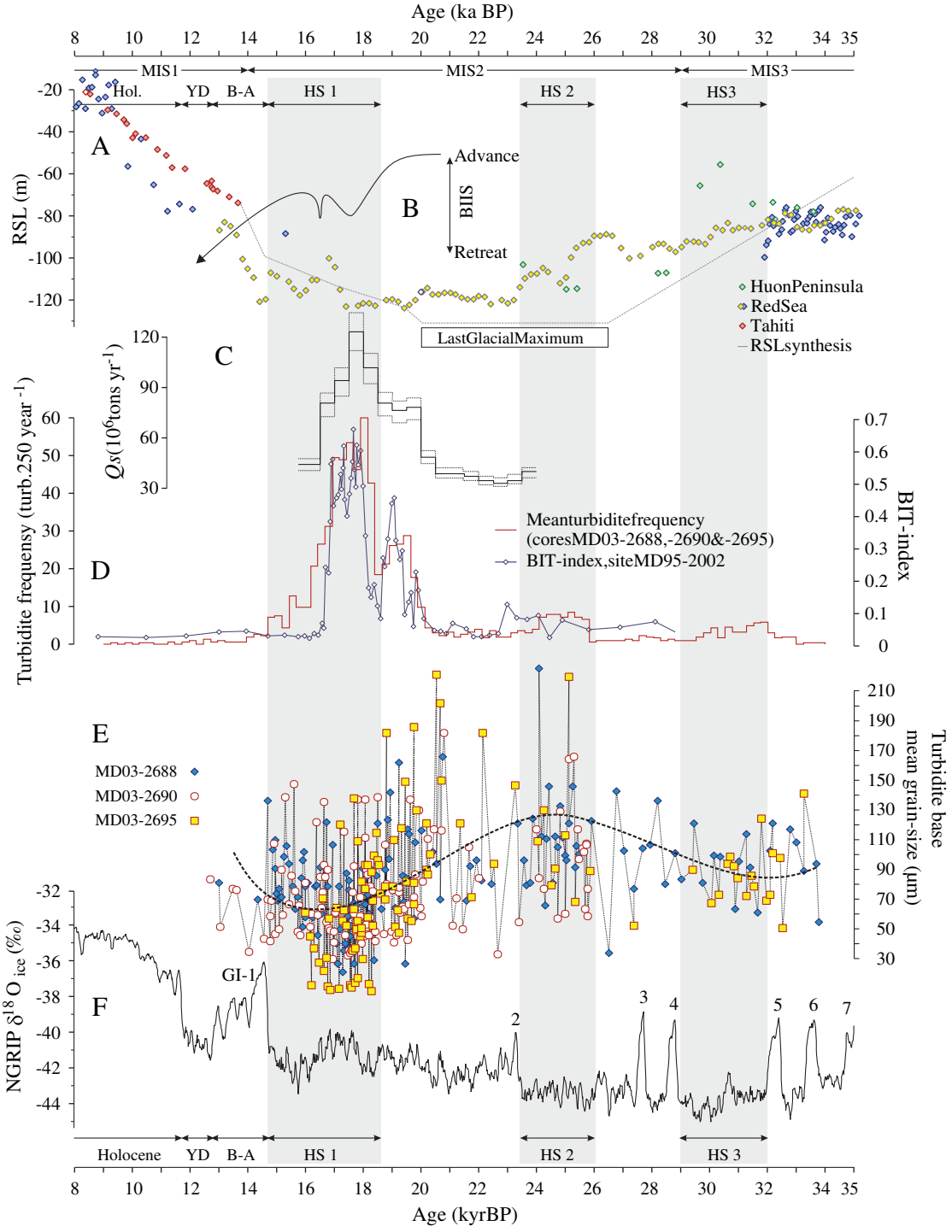

Fig. 8. (A) Relative sea-level (RSL) reconstructions from Tahiti corals (Bard et al., 1996), the Red Sea (Siddall et al., 2003) and the Huon Peninsula (Cutler et al., 2003). The eustatic sea-level time serie is shown as a grey line (Clark et al., 2009). The Last Glacial Maximum is defined from Clark et al. (2009). (B) British Irish Ice Sheet (BIIS) oscillations in the Irish Sea Basin (Toucanne et al., 2008; and references therein); (C) Data-based estimation of the Fleuve Manche sediment load (*Qs* — uncertainties, dashed lines) with a 500-year resolution (Toucanne et al., 2010); (D) Mean turbidite frequency for cores MD03-2690, MD03-2688 and MD03-2695 with a 250-year resolution (red line, this study) and BIT-index at site MD95-2002 (blue line) (Ménot et al., 2006) (see Figs. 1 and 2 for location); (E) Mean grain-size of turbidite bases in cores MD03-2688, MD03-2690 and MD03-2695 (fifth-order polynomial average shown as dashed black line); (F) The NorthGRIP $\delta^{18}O$ profile (GICC05 chronology; Svensson et al., 2008). The Greenland Interstadials are indicated as GI. Marine Isotope Stages (MIS) boundaries according to Lisiecki and Raymo (2005). B–A: Bölling–Alleröd, YD: Younger Dryas. Light grey bands indicate the Heinrich stadials (HS).

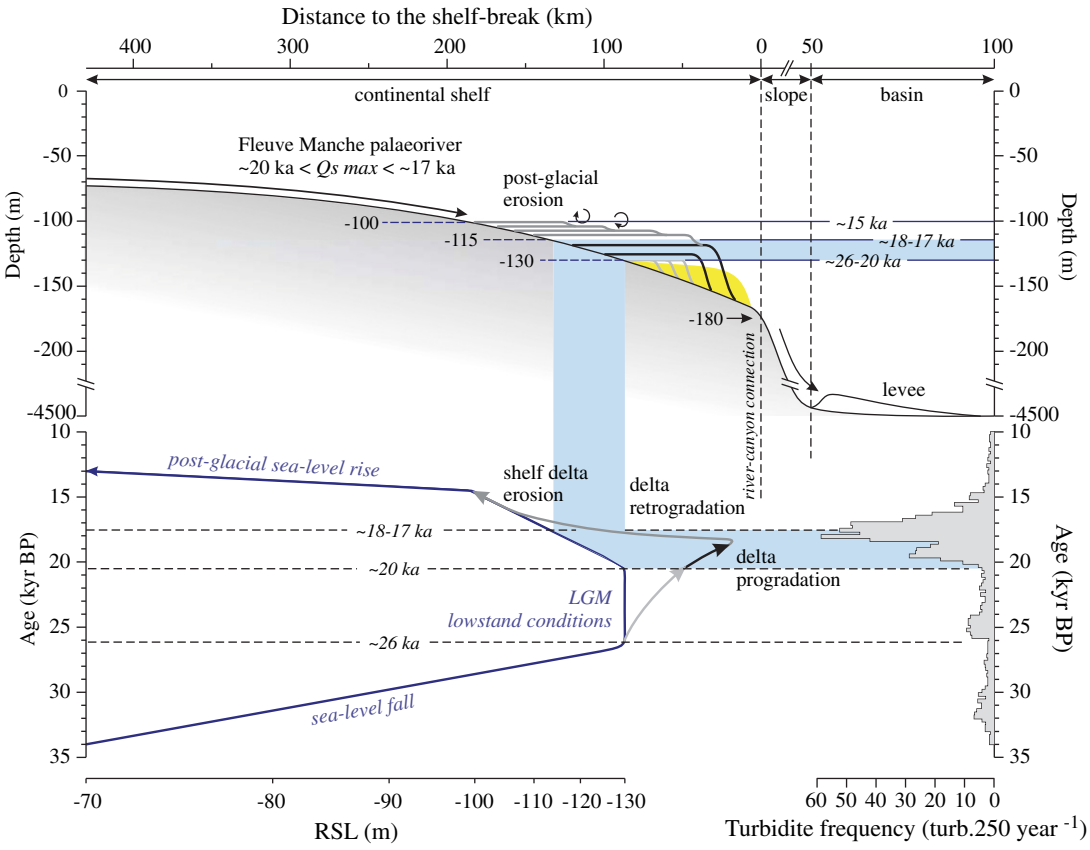

Fig. 9. Conceptual model of sedimentation on the Armorican margin during the LGM (ca. 26.5–20 ka) and the Late Glacial (ca. 20–15 ka). This scenario is based on the estimation of Fleuve Manche palaeoriver discharge (*Qs*; Toucanne et al., 2010), sedimentological criteria from the Armorican shelf (modern position of the Celtic sand banks in yellow; Fig. 2) and the Armorican turbidite system (mean turbidite frequency from cores MD03-2690, MD03-2688 and MD03-2695, with a 250-year resolution; Figs. 2 and 6), and eustatic sea-level fluctuations (RSL: Relative sea-level; Clark et al., 2009). The topographic profile from −70 to −220 m corresponds to the dashed green line drawn in Fig. 2. The combined effect of the isostatic components is that the shelf-break bathymetry on the Armorican margin remained at around −180 m over the studied period (Lambeck, 1997; Törnqvist et al., 2006). During the LGM lowstand and until ca. 18 ka, the progradation of an outer-shelf delta probably occurred in response to the Fleuve Manche sediment load. The latter is known to reach a maximum between ca. 20 and 17 ka (Ménot et al., 2006; Toucanne et al., 2010). This process improved the river–canyon connection and led to the high sediment flux of fine river sediment in the deep depositional system. The development of an outer-shelf delta during this period of time reconciles the conflicting evidence for an outstanding record of the European deglaciation down to a wide drowned shelf (Fig. 2), especially because the abrupt 10 to 20 m rise in sea-level between ca. 20 and 18 ka would led to a rapid shoreline retreat of about 50 km. The delta retrogradation probably occurred at ca. 18–17 ka due to the rapid rise in sea-level and the subsequent gradual decrease of the Fleuve Manche sediment load. The moderate turbidite frequency observed until ca. 15–14 ka probably reflects the erosion of the shelf deposits in response to the rapid landward migration of the shore zone. It is widely accepted that the Celtic sand banks (in yellow in the upper part of the figure) are vestigial tidally remobilised sediments evolving from this palaeodelta (Berné et al., 1998; Scourse et al., 2009).

−180 m on the Armorican margin and, considering the LGM sea-level fall of ca. 120 m and the low slope gradient of the Armorican shelf, we conclude that the drowned shelf was large enough (ca. 100 km wide, Figs. 2 and 9) at that time to store sediment and buffer its delivery to the Armorican turbidite system. The sandy nature of the turbidites deposited onto the Guilcher, Crozon and Audierne levees during the LGM corroborates this hypothesis, likely highlighting a significant winnowing of the fine particles on the continental shelf. Indeed, wave action and currents (i.e. wind driven, tidally induced and density driven flows) transform an initial stock of fine sediments from a river source into a sediment volume of coarser mean grain size in equilibrium with the hydrodynamic conditions (e.g. Black, 1992). Such hydrodynamic conditions would also certainly have provided a strong and effective mechanism for transporting sediment from the shelf to the slope (Pingree and Le Cann, 1989; Mulder et al., 2012). This idea is supported by palaeotidal modelling results, which show that strong tidal pumping of sediments into slope canyon heads on the Armorican outer shelf occurred during the LGM (Scourse et al., 2009). The effectiveness of this process is corroborated by the frequency of glacial turbidites, which is of the same order of magnitude as that calculated on the Var Sedimentary Ridge (e.g. core KNI-23 in Jorry et al., 2011), where the height of the levee was similar to that of the top of the Guilcher, Crozon and Audierne levees (ca. 150 m), at time of maximum sediment discharge of the Var River (Jorry et al., 2011). This result is unexpected considering that, contrary to the Var deep-sea fan, the Armorican turbidite system was not directly connected to the river during the last glacial interval.

Global sea-level was about 40 to 90 m higher during late MIS 3 (i.e. RSL at −40 to −80 m at ca. 35 ka) compared with the LGM (Siddall et al., 2008). This implies that the drowned shelf was more developed at that time than during the LGM (Fig. 9). Consequently, the storage of sediment on the Armorican shelf would be expected to be longer and the winnowing of fine particles more efficient. Indeed, the longer the sediment storage, the more efficient the winnowing (i.e. sediment stock reaches complete equilibrium with the hydrodynamic conditions). For an unchanged sediment source, the sediment stock feeding the depositional system is thus expected to have been coarser during the late MIS 3 than during the LGM. However, an inverse pattern is observed on the sedimentary levees, with thinner and finer-grained turbidites between 35 and 26 ka than during the subsequent 26–20 ka period (Figs. 7 and 8). A first interpretation can be proposed regarding the characteristics of the channelled flows. Considering that coarse-grained flows are usually thinner

than fine-grained flows, the finer-grained turbidites deposited at sites MD03-2690, MD03-2688 and MD03-2695 during the late MIS 3 could originate from coarse-grained turbidity currents from which only the fine-grained well-mixed upper portion is able to spread onto the levees. Coarser levee deposits during the LGM would then have originated from fine-grained turbidity currents of greater thickness, a significant part of the flows spreading onto the overbank surfaces. A second interpretation is that the large, millennial-scale sea-level oscillations dating from MIS 3 (ca. 35 ± 12 m in amplitude, with rates of up to 2 cm year^{-1}; Siddall et al., 2008) shortened the storage of sediment on the Armorican shelf by enhancing the sediment transport to the canyon heads. Contrary to the LGM stable lowstand conditions, these sea-level shifts caused the duration of the wave action and current on the stored sediment to be insufficiently long to produce a complete winnowing of the fine particles. As a result, the sediment feeding the Armorican turbidite system was finer during late MIS 3 than during the LGM, thus leading to finer-grained deposits onto the Guilcher, Crozon and Audierne levees. Additional data, such as sedimentary cores in the depositional-lobe deposits, are needed to answer this question and to learn about the textural characteristics of the sediment stored on the shelf. In any case, it is clear that the sediment supply to the Armorican turbidite system and the Fleuve Manche discharge were both low during the late MIS 3 and the LGM (Ménot et al., 2006; Toucanne et al., 2010), and the drowned shelf acted as a buffer between the Fleuve Manche palaeoriver and the deep Bay of Biscay.

5.2.2. The deglacial period (20–17 ka)

The turbidite sedimentation onto the Guilcher, Crozon and Audierne levees changed dramatically after the LGM. The strong decrease in both the bed thickness and basal grain-size observed between ca. 24 and 18 ka indicates a profound modification of the processes initiating sedimentary density flows in the studied channel–levee systems at the onset of the last deglaciation. The levee growth strongly increased from 30–100 cm ka^{-1} during the LGM to 500–700 cm ka^{-1} around 18–17 ka, and the deposit of an ultra-laminated facies composed of thin and very fine-grained turbidites between 18.3 and 17 ka (i.e. facies 4) indicates there was spillover of very frequent mud-rich flows on the levees (up to ca. 70 events per 250 years; Fig. 6). These mud-rich flows, in addition to the turbid hypopycnal muddy plumes from which originate the peculiar laminated facies described at sites MD95-2002 and MD03-2696 (Toucanne et al., 2009a), were probably triggered by the vigorous, concomitant spring discharges of the Fleuve Manche (i.e. meltwater floods) in response to the increased runoff of the surrounding ice sheets (Zaragosi et al., 2001a; Eynaud et al., 2007; Toucanne et al., 2009a). This is corroborated by the excellent correlation between the evolution of turbidite frequency in each channel–levee system and the evolution at site MD95-2002 of both freshwater algae concentration (Zaragosi et al., 2001a) and BIT (Branched and Isoprenoid Tetraether)-index (Fig. 8), a novel tracer for terrestrial organic carbon fluvially transported in the open ocean (Ménot et al., 2006). Such correlations are unexpected considering the width of the post-LGM shelf (>100 km, Figs. 2 and 9), and the trigger mechanism of the turbidity current remains unclear. Indeed, the very large drowned shelf prevailed from the direct amount of sediment supply to the canyon heads. Considering the shelf physiography and the huge sediment volume deposited by the Fleuve Manche, we assume that a significant lowstand deltaic system have to had developed on the outer shelf as a depocentre of the Fleuve Manche palaeoriver (Fig. 9). It is accepted that the Celtic sand banks originate from this depocentre (Berné et al., 1998; Lericolais et al., 2003; Reynaud et al., 2003; Scourse et al., 2009). The delta progradation probably improved the river–canyon connection, and the numerous deglacial turbidites described on the Guilcher, Crozon and Audierne levees likely evolved either from destabilisation of freshly deposited sediment from the distal part of the prodelta (i.e. sediment failure) or from the direct entrance of sediment-laden freshwater flows (i.e. hyperpycnal flows). The latter process was previously suggested for the Armorican margin by Zaragosi et al. (2001a) and Mulder et al. (2003).

Similar episodes of rapid sediment accumulation related to the last deglaciation (i.e. meltwater intervals) have been recorded in other turbidite systems in the North Atlantic (Kolla and Perlmutter, 1993; Knutz et al., 2002; Skene and Piper, 2003; Tripsanas and Piper, 2008). The Laurentian Fan, off the eastern Canadian continental margin, shows a very similar evolution both in sediment flux and chronology with mud turbidites accumulated onto the levees at very high rates of sedimentation (of the order of 10 m ka^{-1}) between ca. 21 and 17 ka (Skene and Piper, 2003). But a striking difference exists with the Armorican setting because the Laurentian Fan is located off the Laurentian Channel ice-stream, a major outlet of the eastern Laurentide ice-sheet. Physiographically, the Mississippi Fan in the deep Gulf of Mexico is more similar to the Armorican turbidite system, showing a continental-scale river connecting a retreating ice-sheet to a deep depositional system at the end of the last glacial period (Kolla and Perlmutter, 1993). Turbidite sedimentation dramatically increased in the Mississippi Fan ca. 16–13 ka (Kolla and Perlmutter, 1993). Firstly, because the southern part of the Laurentide ice-sheet was rapidly retreating at that time and, secondly, because the increase in meltwater discharges and sediment loads were delivered directly to the Mississippi Fan by means of cross-shelf valleys that are directly connected to the continental slope through a shelf-edge delta (Suter and Berryhill, 1985; Kolla and Perlmutter, 1993; Törnqvist et al., 2006). Indeed, contrary to the Armorican margin, the lowstand shoreline is below the shelf edge in the northern Gulf of Mexico (Törnqvist et al., 2006). These examples from the western North Atlantic strongly support the idea that glacial meltwater discharges could have been delivered directly to the heads of the canyons by the Fleuve Manche palaeoriver during the deglaciation. The development of an outer-shelf delta reconciles the conflicting evidence for an outstanding record of the European deglaciation down to a 100 km wide drowned shelf expected to buffer the delivery of deglacial material to the deep-water area.

5.2.3. The post-glacial period (17–0 ka)

The turbidite frequency at sites MD03-2690, MD03-2688 and MD03-2695 suggests that the sediment inputs to the Armorican turbidite system were less and less frequent after the deglacial episode (Figs. 6, 7 and 8). A strong decrease in accumulation rates occurred on the levees after 17 ka and the turbidite frequency reached a maximum of 5 turbidites per 250 years around 14 ka. The BIT-index at site MD95-2002 shows that the Fleuve Manche discharge fell abruptly at ca. 17 ka and remained very low thereafter (Ménot et al., 2006). However, the turbidite frequency remained significant between 17 and 15 ka and probably reflects the erosion (ravinement) of the shelf deposits (including the lowstand delta) in response to the significant sea-level rise (ca. 30 m) and the rapid landward migration of the shore zone (Bard et al., 1996) (Fig. 9). The sediment input ceased rapidly after 15 ka while the sea-level rose dramatically at that time (Bard et al., 1996, 2010), suggesting that sediment storage increased during the deglacial sea-level rise and the subsequent highstand conditions (Zaragosi et al., 2000; Dennielou et al., 2009). This is corroborated by the significant increase in sediment particle size and thickness of the overspill deposits after the deglacial Fleuve Manche discharge (Figs. 7 and 8), the sediment source for sedimentary flows evolving from direct fine river sediment to remobilisation of winnowed material from the continental shelf. The development of the Celtic Sea sand banks (Berné et al., 1998; Reynaud et al., 2003; Scourse et al., 2009), concomitant shutdown of the sediment delivery in the Celtic Fan (Zaragosi et al., 2000), and sand-rich nature of the rare sedimentary density flows feeding the northern Biscay abyssal plain during the Early Holocene (cores MaKS-03 and MaKS-04; Zaragosi et al., 2001b) all supports this hypothesis.

5.3. Is the Armorican margin a good candidate for climate-driven signal propagation from source to sink?

Toucanne et al. (2008) postulated that the fluctuations of turbidite accumulation on the Guilcher, Crozon and Audierne levees were only forced by fluctuations of the European ice-sheets and the runoff from the Fleuve Manche. The evolution of the turbidite thickness and grain-size at sites MD03-2690, MD03-2688 and MD03-2695, when compared with the evolution of the accumulation rates and turbidite frequency, partly challenges this former interpretation by showing that significant changes in turbidite sedimentation occurred while the sediment supply onto the levees remained constant. This is particularly evident between 35 and 20 ka, when significant variations in the thickness and grain-size of the turbidites were observed. Considering the shelf physiography and the sea-level variability between 35 and 20 ka, these new data suggest that variations in turbidite sedimentation on the levees during this period also reflect variations in accommodation and storage on the shelf. The change in the Fleuve Manche discharge, expected from ca. 35 ka with the glacial advance in the North Sea area (Graham et al., 2010), the increasing periglacial slope activity and sediment production in the northern Alps (Vandenberghe and Pissart, 1993) and the channel belt incision in the Rhine–Meuse system (Busschers et al., 2007) are not recorded in the submarine levees because the drowned shelf acted as a powerful buffer between the European hinterland and the deep-sea sink. Our results may also corroborate recent results suggesting that terrestrial segments of sediment routing systems (i.e. river, floodplain, and river mouth) obscure the expression of high-frequency palaeoenvironmental changes (Jerolmack and Paola, 2010; Armitage et al., 2011a) and that the lag time between climate-driven onshore changes and offshore deposition might reach millions of years in extensive land-to-deep-sea sediment-routing systems (Métivier and Gaudemer, 1999; Castelltort and Van Den Driessche, 2003). Considering the western European drainage alignment and the Armorican turbidite system as a whole, we suggest that for the 35–20 ka period (as well as the 17–0 ka) the western European sediment-routing system was *buffered* (sensu Allen, 2008), as the deep marine depositional environments did not respond to climate-driven terrestrial changes.

This pattern was profoundly different during Termination I, when sediment supply became the main driver for outer-shelf delta and levee growth. Sediment accommodation rapidly shifted from the drowned shelf to the Armorican turbidite system in response to the huge increase in meltwater discharge and sediment load from the Fleuve Manche palaeoriver. The Armorican turbidite system was then directly connected to BIIS, FIS and the Alps glaciers (Fig. 1), as demonstrated by the concomitant changes in the sediment supply onto the levees and the ice-sheet retreat up to the Northern European Lowlands (Rinterknecht et al., 2006; Ehlers et al., 2011). This suggests that the western European sediment-routing system was *reactive* (sensu Allen, 2008) between 20 and 17 ka. It also suggests that turbidite depositional systems can allow us to examine, at least in some specific cases, the landscape response (i.e. erosion, transfer) to climate changes, an hypothesis greatly questioned over the past few years (e.g. Métivier and Gaudemer, 1999; Castelltort and Van Den Driessche, 2003; Jerolmack and Paola, 2010).

6. Conclusions

The detailed sedimentological analysis of cores MD03-2690, MD03-2688 and MD03-2695, through the determination of sedimentary facies and reconstruction of sediment accumulation rates, turbidite frequency, turbidite thickness and grain-size, provides a continuous depositional history of the levees in the Armorican turbidite system (Bay of Biscay, NE Atlantic) over the last 35 ka. The following conclusions can be drawn:

1. Overspilling turbidity currents in the Armorican turbidite system controlled the levee growth from 35 ka to 8 ka, while a slow accumulation of hemipelagic sediment occurred thereafter. This suggests, in agreement with sedimentological evidences from cores retrieved down to the Crozon channel–levee (cores MaKS-03 and MaKS-04; Zaragosi et al., 2001b), that the Armorican turbidite system was inactive (i.e. sediment-starved) during the Holocene sea-level highstand.
2. Sediment accumulation rates and turbidite frequency reveal that, contrary to prediction from the original sequence stratigraphy models, no increase in sediment supply occurred during falling sea-level (35–26 ka) or sea-level lowstand conditions (ca. −120 m during the LGM, 26.5–20 ka). Turbidite fluxes were relatively low onto the levees during this interval. When the results are coupled with modern shelf physiography (shelf-break at ca. −180 m), they show that the drowned shelf was large enough (ca. 100 km wide during the LGM) to store sediment and to buffer sediment delivery to the Armorican turbidite system.
3. Although turbidite fluxes were relatively low between 35 and 20 ka, significant changes in the vertical grain size and bed thickness trends are described on the Guilcher, Crozon and Audierne levees at time of major climate transitions. These changes likely reveals the impact of hydrodynamic and millennial-scale sea-level changes on the quantity and quality of the initial sediment volume transported from the continental shelf to the deep-water area by the turbidity currents.
4. Maximum turbidite flux onto the levees occurred at the onset of Termination 1, from ca. 20 to 17 ka, thus making the Armorican turbidite system a transgression-dominated system. Turbidity currents were triggered by the vigorous discharges of the Fleuve Manche palaeoriver (i.e. meltwater floods) in response to the increased runoff of the BIIS, FIS and Alps glaciers. This, added to the rapid progradation of a large outer-shelf delta, positioned the Armorican turbidite system at the terminus of a *reactive* western European sediment-routing system during the European deglaciation.
5. The Armorican turbidite system, although active during the last glacial interval, is a very unusual depositional system with relatively low sediment flux during (moderate and full) glacial conditions and significant sediment supply restricted to the deglacial interval only. These results emphasise the conclusions drawn by Törnqvist et al. (2006) which predict, based on a geomorphological approach, that the depositional pattern on the Armorican margin is at odds with conventional sequence stratigraphic models. As pointed out by these authors, the Armorican turbidite system is probably a relevant analogue for pre-MPT (i.e. Early Pleistocene and Pliocene) turbidite depositional systems when eustatic sea-level lowstands were −80 to −20 m and sea level was less likely to drop to the shelf edge, thus limiting the sediment supply to the deep-water area.

Precise knowledge about the geological setting and the climate, sea-level and palaeogeographical changes over the studied period have facilitated the interpretation of the sedimentological dataset, allowing the isolation of the forcing factors affecting turbidite sedimentation. Such interpretations are usually difficult in fossil systems due to the difficulties of precisely linking oscillations of the sedimentological parameters with (potentially unknown) climate-induced changes. The conclusions drawn in this study require testing, particularly by channel- and depositional-lobe-based observations. However, our study definitely provides useful information regarding the forcing factors controlling levee growth in modern as well as fossil turbidite systems.

Acknowledgements

The authors are very grateful to G. Chabaud, J. Saint Paul, O. Ther (University Bordeaux 1), G. Floch, R. Kerbrat and M. Rovere (IFREMER) for their technical support; they also thank the crew and

scientific teams of the MD133-SEDICAR cruise (R/V *Marion Dufresne II*) for the recovery of the long piston cores; the programme ARTEMIS (INSU-CNRS) for the use of ^{14}C measurement facilities; S. Charrier, E. Gautier and M. Veslin for their help with GIS map production; M. Voisset for access to the ValidOP acoustic dataset; Helen McCombie-Boudry for English improvements. The authors finally acknowledge E. Tripsanas, an anonymous reviewer and the Editor D.J.W. Piper for their helpful comments, which greatly improved this paper.

References

Allen, P.A., 2008. Time scales of tectonic landscapes and their sediment routing systems. Geological Society of London, Special Publications 296, 7–28.
Armitage, J.J., Duller, R.A., Whittaker, A.C., Allen, P.A., 2011a. Transformation of tectonic and climatic signals from source to sedimentary archive. Nature Geoscience 4, 231–235.
Armitage, J.J., Duller, R., T., D.J., Whittaker, A., Allen, P.A., 2011b. Climate signals lost and found in the sediment archive. Geophysical Research Abstracts 8 EGU2011-3591.
Auffret, G., Zaragosi, S., Dennielou, B., Cortijo, E., Van Rooij, D., Grousset, F., Pujol, C., Eynaud, F., Siegert, M., 2002. Terrigenous fluxes at the Celtic margin during the last glacial cycle. Marine Geology 188 (1–2), 79–108.
Bard, E., Hamelin, B., Arnold, M., Montaggioni, L., Cabioch, G., Faure, G., Rougerie, F., 1996. Deglacial sea-level record from Tahiti corals and the timing of global meltwater discharges. Nature 382, 241–244.
Bard, E., Hamelin, B., Delanghe-Sabatier, D., 2010. Deglacial meltwater pulse 1B and Younger Dryas sea levels revisited with boreholes at Tahiti. Science 327, 1235–1237.
Barker, S., Diz, P., Vautravers, M.J., Pike, J., Knorr, G., Hall, I.R., Broecker, W.S., 2009. Interhemispheric Atlantic seesaw response during the last deglaciation. Nature 457, 1097–1103.
Berné, S., Lericolais, G., Marsset, T., Bourillet, J.F., De Batist, M., 1998. Erosional offshore sand ridges and lowstand shorefaces; examples from tide- and wave-dominated environments of France. Journal of Sedimentary Research 68 (4), 540–555.
Black, K.P., 1992. Evidence of the importance of deposition and winnowing of surficial sediments at a continental shelf-scale. Journal of coastal research 8 (2), 319–331.
Bouma, A.H., 2001. Fine-grained submarine fans as possible recorders of long- and short-term climatic changes. Global and Planetary Change 28 (1–4), 85–91.
Bourillet, J.F., Reynaud, J.Y., Baltzer, A., Zaragosi, S., 2003. The "Fleuve Manche": the submarine sedimentary features from the outer shelf to the deep-sea fans. Journal of Quaternary Science 18 (3–4), 261–282.
Bourillet, J.F., Zaragosi, S., Mulder, T., 2006. The French Atlantic margin and the deep sea submarine systems. Geo-Marine Letters 26 (6), 311–315.
Bourillet, J.F., Damy, G., Dussud, L., Sultan, N., Woerther, P., Migeon, S., 2007. Behaviour of a piston corer from accelerometers and new insights on quality of the recovery. Proceedings of the 6th International Offshore Site Investigation and Geotechnics Conference: Confronting New Challenges and Sharing Knowledge, 11–13 September 2007, London, UK.
Busschers, F.S., Kasse, C., Van Balen, R.T., Vandenberghe, J., Cohen, K.M., Weerts, H.J.T., Wallinga, J., Johns, C., Cleveringa, P., Bunnik, F.P.M., 2007. Late Pleistocene evolution of the Rhine–Meuse system in the southern North-Sea Basin: imprints of climate change, sea-level oscillation and glacio-isostacy. Quaternary Science Reviews 26 (25–28), 3216–3248.
Castelltort, S., Van Den Driessche, J., 2003. How plausible are high-frequency sediment supply-driven cycles in the stratigraphic record? Sedimentary Geology 157 (1–2), 3–13.
Clark, P.U., Dyke, A.S., Shakun, J.D., Carlson, A.E., Clark, J., Wohlfarth, B., Mitrovica, J.X., Hostetler, S.W., McCabe, A.M., 2009. The Last Glacial Maximum. Science 325, 710–714.
Clark, C.D., Hughes, A.L.C., Greenwood, S.L., Jordan, C., Sejrup, H.S., in press. Pattern and timing of retreat of the last British-Irish Ice Sheet. Quaternary Science Reviews. doi:10.1016/j.quascirev.2010.07.019.
Covault, J.A., Graham, S.A., 2010. Submarine fans at all sea-level stands: tectono-morphologic and climatic controls on terrigenous sediment delivery to the deep sea. Geology 38, 939–942.
Covault, J.A., Romans, B.W., Fildani, A., McGann, M., Graham, S.A., 2010. Rapid climatic signal propagation from source to sink in a southern California sediment-routing system. The Journal of Geology 118, 247–259.
Cutler, K.B., Edwards, R.L., Taylor, F.W., Cheng, H., Adkins, J., Gallup, C.D., Cutler, P.M., Burr, G.S., Bloom, A.L., 2003. Rapid sea-level fall and deep-ocean temperature change since the last interglacial period. Earth and Planetary Science Letters 206, 253–271.
Dennielou, B., Huchon, A., Beaudouin, C., Berné, S., 2006. Vertical grain-size variability within a turbidite levee: autocyclicity or allocyclicity? A case study from the Rhone neofan, Gulf of Lions, Western Mediterranean. Marine Geology 234 (1–4), 191–213.
Dennielou, B., Jallet, L., Sultan, N., Jouet, G., Giresse, P., Voisset, M., Berné, S., 2009. Post-glacial persistence of turbiditic activity with the Rhone deep-sea turbidite system (Gulf of Lions, Western Mediterranean): linking the outer shelf and the basin sedimentary records. Marine Geology 257 (1–4), 65–86.
Denton, G.H., Anderson, R.F., Toggweiler, J.R., Edwards, R.L., Schaefer, J.M., Putnam, A.E., 2010. The Last Glacial Termination. Science 328, 1652–1656.
Droz, L., Auffret, G.A., Savoye, B., Bourillet, J.F., 1999. L'éventail profond de la marge Celtique: stratigraphie et évolution sédimentaire. C.R. Acad. Sci. Paris 328, 173–180.
Ehlers, J., Gibbard, P.L., Hughes, P.D., 2011. Quaternary Glaciations — Extent and Chronology, 15. Elsevier, Amsterdam. 1126 pp.
Eynaud, F., Zaragosi, S., Scourse, J.D., Mojtahid, M., Bourillet, J.F., Hall, I.R., Penaud, A., Locascio, M., Reijonen, A., 2007. Deglacial laminated facies on the NW European continental margin: the hydrographic significance of British Ice sheet deglaciation and Fleuve Manche paleoriver discharges. Geochemistry, Geophysics, Geosystems 8. doi:10.1029/2006GC001496.
Gibbard, P.L., 1988. The history of great northwest European rivers during the past three millions years. Phil. Trans. R. Soc. Lond. B318, 559–602.
Graham, A.G.C., Lonergan, L., Stoker, M., 2010. Depositional environments and chronology of Late Weichselian glaciation and deglaciation in the central North Sea. Boreas 39 (3), 471–491.
Grousset, F.E., Pujol, C., Labeyrie, L., Auffret, G., Boelaert, A., 2000. Were the North Atlantic Heinrich events triggered by the behavior of the European ice sheets? Geology 28 (2), 123–126.
Hiscott, R.N., Hall, F.R., Pirmez, C., 1997. Turbidity current overspill from the Amazon Channel: texture of the silt/sand load, paleoflow from anisotrophy of magnetic susceptibility, and implications for flow processes. In: Flood, R.D., Piper, D.J.W., Klaus, A., Peterson, L.C. (Eds.), Proceedings of the ODP Sci. Results 155. Ocean Drilling Program, College Station, TX, pp. 53–78.
Jerolmack, D.J., Paola, C., 2010. Shredding of environmental signals by sediment transport. Geophysical Research Letters 37, L19401. doi:10.1029/2010GL044638.
Jorry, S.J., Jégou, I., Emmanuel, L., Silva Jacinto, R., Savoye, B., 2011. Turbiditic levee deposition in response to climate changes: the Var Sedimentary Ridge (Ligurian Sea). Marine Geology 279 (1–4), 148–161.
Khripounoff, A., Vangriesheim, A., Crassous, P., Etoubleau, J., 2009. High frequency of sediment gravity flow events in the Var submarine canyon (Mediterranean Sea). Marine Geology 263 (1–4), 1–6.
Knutz, P.C., Jones, E.J.W., Austin, W.E.N., van Weering, T.C.E., 2002. Glacimarine slope sedimentation, contourite drifts and bottom current pathways on the Barra Fan, UK North Atlantic margin. Marine Geology 188 (1–2), 129–146.
Kolla, V., Perlmutter, M., 1993. Timing of turbidite sedimentation on the Mississippi Fan. American Association of Petroleum Geologists Bulletin 77, 1129–1141.
Laberg, J.S., Andreassen, K., Vorren, T.O., 2011. Late Cenozoic erosion of the high-latitude southwestern Barents Sea shelf revisited. Geological Society of America Bulletin 124 (1–2), 77–88.
Lambeck, K., 1997. Sea-level change along the French Atlantic and channel coasts since the time of the Last Glacial Maximum. Palaeogeography, Palaeoclimatology, Palaeoecology 129, 1–22.
Le Roy, P., Gracia-Garay, C., Guennoc, P., Bourillet, J.F., Reynaud, J.Y., Thinon, I., Kervevan, P., Paquet, F., Menier, D., Bulois, C., 2011. Cenozoic tectonics of the Western Approaches Channel basins and its control of local drainage systems. Bulletin de la Societe Geologique de France 182, 451–463.
Le Suavé, R., Bourillet, J.F., Coutelle, A., 2000. La marge nord du golfe de Gascogne. Connaissances générales et apport des nouvelles synthèses de données multifaisceaux. Synthèse bathymétrique et imagerie acoustique de la zone économique exclusive Atlantique Nord-Est, Ed. IFREMER, Plouzané. pp 55.
Lericolais, G., Guennoc, P., Auffret, J.P., Bourillet, J.F., Berné, S., 1996. Detailed survey of the western end of the Hurd Deep (English Channel): new facts for a tectonic origin. In: De Batist, M., Jacobs, P. (Eds.), Geology of Siliciclastic Shelf Seas: Special publication, Geological Society, London, pp. 203–215.
Lericolais, G., Auffret, J.P., Bourillet, J.F., 2003. The Quaternary Channel River: seismic stratigraphy of its palaeo-valleys and deeps. Journal of Quaternary Science 18 (3–4), 245–260.
Lisiecki, L.E., Raymo, M.E., 2005. A Pliocene–Pleistocene stack of 57 globally distributed benthic $\delta^{18}O$ records. Paleoceanography 20, PA1003. doi:10.1029/2004PA001071.
Manley, L.P., Pirmez, C., Busch, W., Cramp, A., 1997. Grain-size characterization of Amazon fan deposits and comparison to seismic facies units. In: Flood, R.D., Piper, D.J.W., Klaus, A., Peterson, L.C. (Eds.), Proceedings of the ODP, Sci. Results, 155. Ocean Drilling Program, College Station, TX, pp. 35–52.
Mansor, S., 2004. Faciès sismique et architecture du système turbiditique Armoricain. Unpublished Master thesis, University of Brest, pp. 30.
Mas, V., Mulder, T., Dennielou, B., Schmidt, S., Khripounoff, A., Savoye, B., 2010. Multi-scale spatio-temporal variability of sedimentary deposits in the Var turbidite system (North-Western Mediterranean Sea). Marine Geology 275 (1–4), 37–52.
Menier, D., Reynaud, J.Y., Proust, J.-N., Guillocheau, F., Guennoc, P., Tessier, B., Bonnet, S., Goubert, E., 2006. Inherited fault control on the drainage pattern and infilling sequences of late glacial incised valleys, SE coast of Brittany, France. S.E.P.M. (Society for sedimentary Geology) Special Publication, 85, pp. 37–55.
Ménot, G., Bard, E., Rostek, F., Weijers, J.W.H., Hopmans, E.C., Schouten, S., Sinninghe Damsté, J.S., 2006. Early reactivation of European rivers during the last deglaciation. Science 313, 1623–1625.
Métivier, F., Gaudemer, Y., 1999. Stability of output fluxes of large rivers in south and east Asia during the last 2 million years: implications on floodplain processes. Basin Research 11 (4), 293–303.
Mulder, T., Syvitski, J.P.M., 1996. Climatic and morphologic relationships of rivers: implications of sea-level fluctuations on river loads. Journal of Geology 104, 509–523.
Mulder, T., Syvitski, J.P.M., Migeon, S., Faugères, J.C., Savoye, B., 2003. Marine hyperpycnal flows: initiation, behavior and related deposits. A review. Marine and Petroleum Geology 20 (6–8), 861–882.
Mulder, T., Zaragosi, S., Garlan, T., Mavel, J., Cremer, M., Sottolichio, A., Sénéchal, N., Schmidt, S., 2012. Present deep-submarine canyons activity in the Bay of Biscay (NE Atlantic). Marine Geology 295–298, 113–127.
Nakajima, T., Itaki, T., 2007. Late Quaternary terrestrial climatic variability recorded in deep-sea turbidites along the Toyama Deep-Sea Channel, central Japan Sea. Palaeogeography, Palaeoclimatology, Palaeoecology 247 (1–2), 162–179.

Normark, W.R., Posamentier, H., Mutti, E., 1993. Turbidite systems: state of the art and future directions. Reviews of Geophysics B31, 91–116.
Pingree, R.D., Le Cann, B., 1989. Celtic and Armorican slope and shelf residual currents. Continental Shelf Research 23, 303–338.
Posamentier, H.W., Vail, P.R., 1988. Eustatic controls on clastic deposition II — sequence and systems tract models. In: Wilgus, Ch.K. et al. (Eds.), Sea-level changes: an integrated approach. Soc. Econ. Paleontol. Mineral. Spec. Publ. 42, 125–154.
Reading, H.G., Richards, M., 1994. Turbidite systems in deep-water basin margins classified by grain size and feeder system. Bulletin of the American Association of Petroleum Geologists 78 (5), 792–822.
Reynaud, J.Y., Tessier, B., Proust, J.N., Dalrymple, R.W., Bourillet, J.F., De Batist, M., Lericolais, G., Berné, S., Marsset, T., 1999. Architecture and sequence stratigraphy of a late Neogene incised valley at the shelf margin, southern Celtic Sea. Journal of Sedimentary Research 69 (2), 351–364.
Reynaud, J.Y., Tessier, B., Auffret, J.P., Berné, S., de Batist, M., Marsset, T., Walker, P., 2003. The offshore Quaternary sediment bodies of the English Channel and its Western Approaches. Journal of Quaternary Science 18, 361–371.
Rinterknecht, V.R., Clark, P.U., Raisbeck, G.M., Yiou, F., Bitinas, A., Brook, E.J., Marks, L., Zelcs, V., Lunkka, J.P., Pavlovskaya, I.E., Piotrowski, J.A., Raukas, A., 2006. The last deglaciation of the southeastern sector of the Scandinavian ice sheet. Science 311 (5766), 1449–1452.
Sadler, P.M., 1982. Bed-thickness and grain-size of turbidites. Sedimentology 29, 37–51.
Scourse, J., Uehara, K., Wainwright, A., 2009. Celtic Sea linear tidal sand ridges, the Irish Sea Ice Stream and the Fleuve Manche: palaeotidal modelling of a transitional passive margin depositional system. Marine Geology 259 (1–4), 102–111.
Sejrup, H.P., Hjelstuen, B.O., Dahlgren, K.I.T., Haflidason, H., Kuijpers, A., Nygard, A., Praeg, D., Stoker, M.S., Vorren, T.O., 2005. Pleistocene glacial history of the NW European continental margin. Marine and Petroleum Geology 22 (9–10), 1111–1129.
Siddall, M., Rohling, E.J., Almogi-Labin, A., Hemleben, C., Meischner, D., Scheizmer, I., Smeed, D.A., 2003. Sea-level fluctuations during the last glacial cycle. Nature 423, 853–858.
Siddall, M., Rohling, E.J., Thompson, W.G., Waelbroeck, C., 2008. Marine isotope stage 3 sea level fluctuations: data synthesis and new outlook. Reviews of Geophysics 46, RG4003. doi:10.1029/2007RG000226.
Skene, K.I., Piper, D.J.W., 2003. Late Quaternary stratigraphy of Laurentian Fan: a record of events off the eastern Canadian continental margin during the last deglacial period. Quaternary International 99–100, 135–152.
Skene, K.I., Piper, D.J.W., Hill, P.R., 2002. Quantitative analysis of variations in depositional sequence thickness from submarine channel levees. Sedimentology 49, 1411–1430.
Skinner, L.C., McCave, I.N., 2003. Analysis and modelling of gravity- and piston coring based on soil mechanics. Marine Geology 199 (1–2), 181–204.
Stow, D.A.V., Piper, D.J.W., 1984. Deep-water fine-grained sediments: facies model. Fine-grained sediments: deep-water processes and facies. Geological Society Special Publication 15, 611–645.
Stow, D.A.V., Howell, D.G., Nelson, H.C., 1985. Sedimentary, tectonic, and sea-level controls. In: Bouma, A.H., Normark, W.R., Barnes, N.E. (Eds.), Submarine Fans and Related Turbidite Systems. Springer, New-York, pp. 15–22.
Straub, K.M., Mohrig, D., 2008. Quantifying the morphology and growth of levees in aggrading submarine channels. Journal of Geophysical Research 113, F03012. doi:10.1029/2007JF000896.
Suter, J.R., Berryhill, H.L., 1985. Late Quaternary shelf margin deltas, Northwest Gulf of Mexico. American Association of Petroleum Geologists Bulletin 69, 77–91.
Svensson, A., Andersen, K.K., Bigler, M., Clausen, H.B., Dahl-Jensen, D., Davies, S.M., Johnsen, S.J., Muscheler, R., Parrenin, F., Rasmussen, S.O., Röthlisberger, R., Seierstad, I., Steffensen, J.P., Vinther, B.M., 2008. A 60,000 year Greenland stratigraphic ice core chronology. Climate of the Past 4, 47–57.
Talling, P.J., 2001. On the frequency distribution of turbidite thickness. Sedimentology 48, 1297–1329.
Törnqvist, T.E., Wortman, S.R., Mateo, Z.R.P., Milne, G.I., Swenson, J.B., 2006. Did the last sea level lowstand always lead to cross-shelf valley formation and source-to-sink sediment flux? Journal of Geophysical Research 111, F04002. doi:10.1029/2005JF000425.
Toucanne, S., Zaragosi, S., Bourillet, J.F., Naughton, F., Cremer, M., Eynaud, F., Dennielou, B., 2008. Activity of the turbidite levees of the Celtic–Armorican margin (Bay of Biscay) during the last 30,000 years: imprints of the last European deglaciation and Heinrich events. Marine Geology 247 (1–2), 84–103.
Toucanne, S., Zaragosi, S., Bourillet, J.F., Cremer, M., Eynaud, F., Van Vliet Lanoë, B., Penaud, A., Fontanier, C., Turon, J.L., Cortijo, E., Gibbard, P., 2009a. Timing of massive 'Fleuve Manche' discharges over the last 350 kyr: insights into the European Ice Sheet oscillations and the European drainage network from MIS 10 to 2. Quaternary Science Reviews 28, 1238–1256.
Toucanne, S., Zaragosi, S., Bourillet, J.F., Gibbard, P.L., Eynaud, F., Giraudeau, J., Turon, J.L., Cremer, M., Cortijo, E., Martinez, P., Rossignol, L., 2009b. A 1.2 My record of glaciation and fluvial discharges from the West European Atlantic margin. Quaternary Science Reviews 28, 2974–2981.
Toucanne, S., Zaragosi, S., Bourillet, J.F., Marieu, V., Cremer, M., Kageyama, M., Van Vliet Lanoë, B., Eynaud, F., Turon, J.L., Gibbard, P.L., 2010. The first estimation of Fleuve Manche palaeoriver discharge during the last deglaciation: evidence for Fennoscandian ice sheet meltwater flow in the English Channel ca 20–18 ka ago. Earth and Planetary Science Letters 290, 459–473.
Tripsanas, E.K., Piper, D.J.W., 2008. Late Quaternary stratigraphy and sedimentology of Orphan Basin: implications for meltwater dispersal in the southern Labrador Sea. Palaeogeography, Palaeoclimatology, Palaeoecology 260 (3–4), 521–539.
Vandenberghe, J., Pissart, A., 1993. Permafrost changes in Europe during the Last Glacial. Permafrost and Periglacial Processes 4, 121–135.
Zaragosi, S., Auffret, G.A., Faugeres, J.C., Garlan, T., Pujol, C., Cortijo, E., 2000. Physiography and recent sediment distribution of the Celtic Deep-Sea Fan, Bay of Biscay. Marine Geology 169 (1–2), 207–237.
Zaragosi, S., Eynaud, F., Pujol, C., Auffret, G.A., Turon, J.L., Garlan, T., 2001a. Initiation of the European deglaciation as recorded in the northwestern Bay of Biscay slope environments (Meriadzek Terrace and Trevelyan Escarpment): a multi-proxy approach. Earth and Planetary Science Letters 188 (3–4), 493–507.
Zaragosi, S., Le Suavé, R., Bourillet, J.F., Auffret, G., Faugères, J.C., Pujol, C., Garlan, T., 2001b. The deep-sea Armorican depositional system (Bay of Biscay), a multiple source, ramp model. Geo-Marine Letters 20 (4), 219–232.
Zaragosi, S., Bourillet, J.F., Eynaud, F., Toucanne, S., Denhard, B., Van Toer, A., Lanfumey, V., 2006. The impact of the last European deglaciation on the deep-sea turbidite systems of the Celtic–Armorican margin (Bay of Biscay). Geo-Marine Letters 26 (6), 317–329.